

Updated 2D Tracker TSIM Design for Central Drift Chamber(CDC) at Belle-II

M.C. Chang, K.Y. Chen*, Z.X Chen
FU-JEN CATHOLIC UNIVERSITY

July 3, 2015

Abstract

The functions of Belle-II CDC is to detect charged particles from particle interactions. This kind of detector is crucial among many sub-detectors.

A simple idea of comprehending CDC is: the CDC detects charged tracks using sense wires and field wires.

My task is to simulate the 2d track reconstruction algorithm for CDC readout electronics. This algorithm should fit the performance in the FPGA chip as well. In my thesis, I introduce the algorithm and the design of my trigger simulation program (TSIM).

TSim is a trigger simulator developed for Belle experiment. TSim has been quite useful in studying trigger performance in the beginning of the experiment. In the case of pipelined trigger system, it works well in debugging the VHDL codes.

Keyword: KEK, Belle II, Central Drift Chamber (CDC), 2D Track Reconstruction, Hough Transformation, Clustering, TSIM.

Contents

0.1	The Belle and Belle-II Experiment	1
0.2	The Central Drift Chamber in Belle and Belle-II	3
0.3	The Readout Electronics of the CDC	9
1	The CDC Trigger System	13
1.1	Introduction	13
1.2	The Front-end and the Merger	15
1.3	The Track Segment Finder (TSF)	16
1.4	The 2D and 3D tracker	17
2	The Hough Voting for 2D Tracker	19
2.1	Hough Transform	19
2.2	Circle Hough Transform	19
2.3	Arcs to mesh	22
3	The Peak Finding for 2D Full and Short Tracker	27
3.1	Hough Cell Clusters	27
3.2	Finding the Regions	28
3.3	Center of Cluster	30
3.4	Mesh Size	31

3.5	FPGA Algorithm	33
3.6	The relation among Pattern I	34
3.7	The relation among Pattern II	35
3.8	Center of Cluster	39
3.9	Efficiency in 2D logic	41
4	The Fitter for 2D Full Tracker	43
4.1	Transforming track segment coordinates	43
4.2	2D fitter	44
4.3	Transforming back 2D fitter results	46
4.4	Classes for Cpp to VHDL	47
4.5	Histogram of Pt and Phi	47
5	Summary	50

List of Figures

1	The luminosity record of the Belle experiment is shown.	3
2	This is a picture of KEK, Japan.	4
3	This is a schematic plot of SuperKEKB (left) and Belle-II detector(right).	5
4	Belle-II logo.	6
5	The Belle-II organization.	7
6	The home towns of joined Belle-II collaborators are labelled in the world map.	8
7	Wire Conguration of the Belle CDC (a) and the Belle-II CDC (b). The filled circle shows an axial wire and the open circle shows a stereo wire.	9
1.1	The parameter of Belle and Belle-II CDC super layers .	14
1.2	The location of CDC super layers	14
1.3	Schematic of the Front-End structure	16
1.4	Schematic of the Merger structure	16
2.1	Schematic view of the right-handed and left-handed circles in the CDC x-y plane.	20
2.2	In the Hough plane	22

2.3	Five wire hits in x-y plane.	23
2.4	Five arcs in Hough Plus and Minus plane.	24
2.6	The idea of transforming the arcs into meshes.	24
2.5	The cross point in the Hough plane means that 5 points are in the same track circle.	25
2.7	An example of transforming the arcs into meshes in TSIM.	25
2.8	After we have the TSFs connected to Hough cells, we can connect the Hough cells in the same position in each super layer. We use AND logic for this superposition. .	26
3.1	The connected hit cells in the Hough Plane are called clusters.	27
3.2	The range of cell neighbors.	29
3.3	Searching process of clusters.	29
3.4	An example of the results after clustering.	30
3.5	Some tracks are very close to each other, an example is shown here.	31
3.6	We allow the neighbor cells are within a 2×3 region. Two allowed neighbor cases are shown here.	32
3.9	Optimized Hough Plane	32
3.7	We update the neighbor scanning region to solve the very-close-tracks problem.	33
3.8	Here shows the difference between previous cluster neigh- boring and updated neighboring.	34
3.10	A Pattern I	34
3.11	The relation between Pattern I and Hough plane. . . .	35

3.12	An example of Pattern II	36
3.13	The hitted rate in the C, F, and I in the Pattern II . .	36
3.14	The relation comparsion between Pattern I	39
3.15	Use the selection rules and decide the center of the Pat- tern II.	40
3.16	Use the selection rules and decide the center of the Pat- tern I.	41
3.17	An efficiency of finding the track.	42
4.1	An example of track segment coordinate.	43
4.2	The histogram of Pt. In each case, we generated 1,000 times. The momentum is from 0.4 to 5.0 GeV.	47
4.3	The histogram of Pt. In each case, we generated 1,000 times. The momentum is from 0.4 to 5.0 GeV.	48
4.4	The resolution of Pt. The momentum is generated from 0.4 to 5.0 GeV.	49
4.5	The histogram of Phi. In each case, we generated 1,000 times. The momentum is from 0.4 to 5.0 GeV	49

0.1 The Belle and Belle-II Experiment

The Belle experiment was operated at a Japanese High-Energy Accelerator Research Organization, named KEK [1]. In KEK, an accelerator KEKB and a detector Belle were build-up for Belle experiment.

The KEKB was a 3 km circumference asymmetric electron–positron collider and operated during 1998 to 2010. It reached the world record

in instantaneous luminosity of $2.11 \times 10^{34} \text{ cm}^{-2}\text{s}^{-1}$. The Figure 1 shows the luminosity record of Belle experiment.

The electron–positron beam energies were chosen to mainly produce B -mesons. This was the reason for Belle experiment also called a B -factory. A picture of KEK is shown in the Figure 2.

The Belle experiment analysed the B - and anti- B mesons precisely. It confirmed the CP -violation as described by the theory of Kobayashi and Maskawa, the KM mechanism [2].

In 2008, Makoto Kobayashi and Toshihide Maskawa, who both were awarded the Nobel prize in physics [3]. The CP -violation is believed to be one of the origins of matter and anti-matter asymmetry in our present universe. However, the measured CP -violation is not enough to explain the matter and anti-matter asymmetry. Therefore, a deeper understanding is required.

The SuperKEKB is an upgrade project at KEK. The goal is to increase the instantaneous luminosity by a factor of 40, to $8 \times 10^{35} \text{ cm}^{-2}\text{s}^{-1}$. This upgraded B -factory, named as Belle-II experiment [4], will explore the New Physics beyond the Standard Model. For LHC, it can provide a probe of the TeV mass scale. For SuperKEKB, it can provide high-precision measurements of rare decays and CP -violation in heavy quarks and leptons. Both of LHC and SuperKEKB are unique for New Physics studies. A schematic plot of SuperKEKB and Belle-II detector is shown in the Figure 3. The Belle-II logo is shown in the Figure 4.

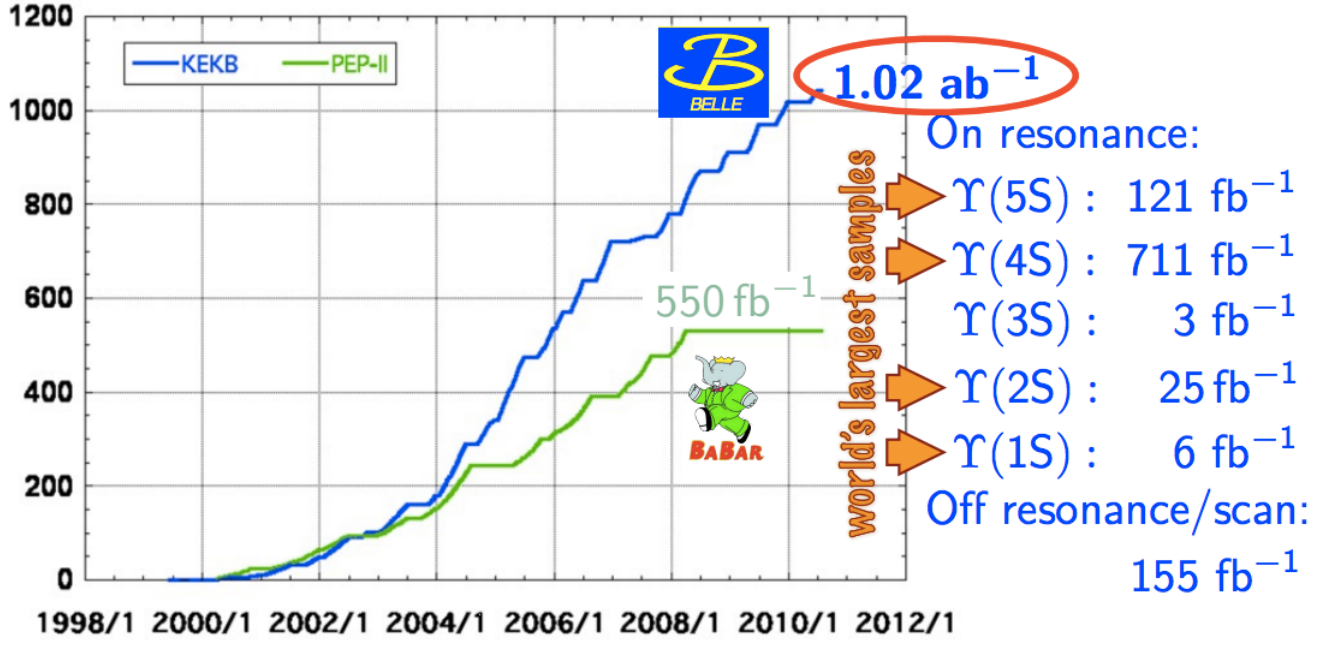


Figure 1: The luminosity record of the Belle experiment is shown.

0.2 The Central Drift Chamber in Belle and Belle-II

The detector, Belle, was located in the KEKB accelerator ring, at the point where the electron and positron beams intersect. The Belle-II detector will sit at the exact same position on the upgraded version of KEKB, the SuperKEKB.

The Belle-II detector will be a large-solid-angle magnetic spectrometer consisting of inner vertex detectors with pixels (PXD) and silicon strips (SVD), a central drift chamber (CDC), a barrel-like arrangement of time-of-propagation counters (TOP), an array of ring-image Cherenkov counters (ARICH), an electromagnetic calorimeter (ECL), and a K_L -and-muon detector (KLM).

The Belle and Belle-II Central Drift Chamber (CDC) detect charged

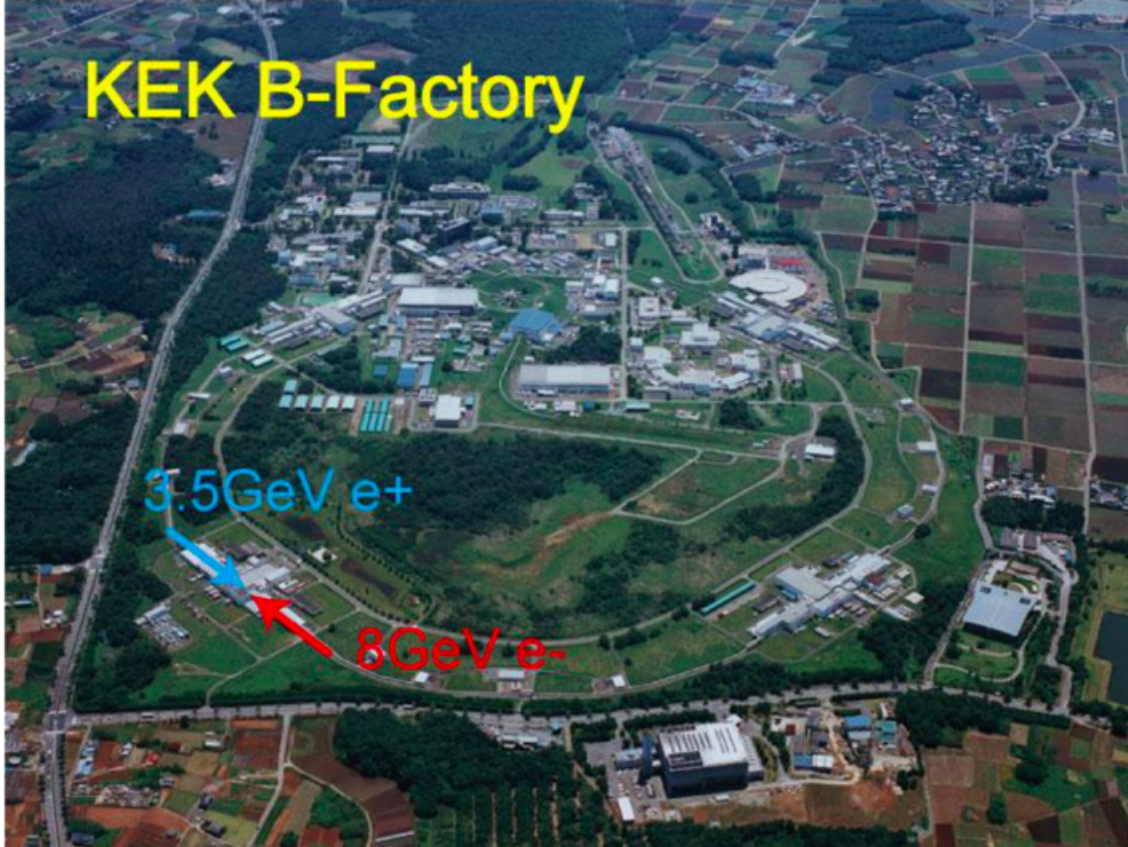


Figure 2: This is a picture of KEK, Japan.

particles resulting from particle interactions. This kind of detector is crucial among many sub-detectors. If without the CDC, it would make no sense to take data from other sub-detectors in Belle and Belle-II.

Designing and constructing the CDC is complex. But a simple idea of understanding CDC is: the CDC detects charged tracks using metal wires [5].

When particles pass through a helium based gas mixture inside the chamber, they ionize the gas molecules, knocking out electrons. An electric field is created by applying high voltage on sense wires strung across the chamber. The field causes electrons to accelerate towards the wires. These electrons knock out additional electrons from the

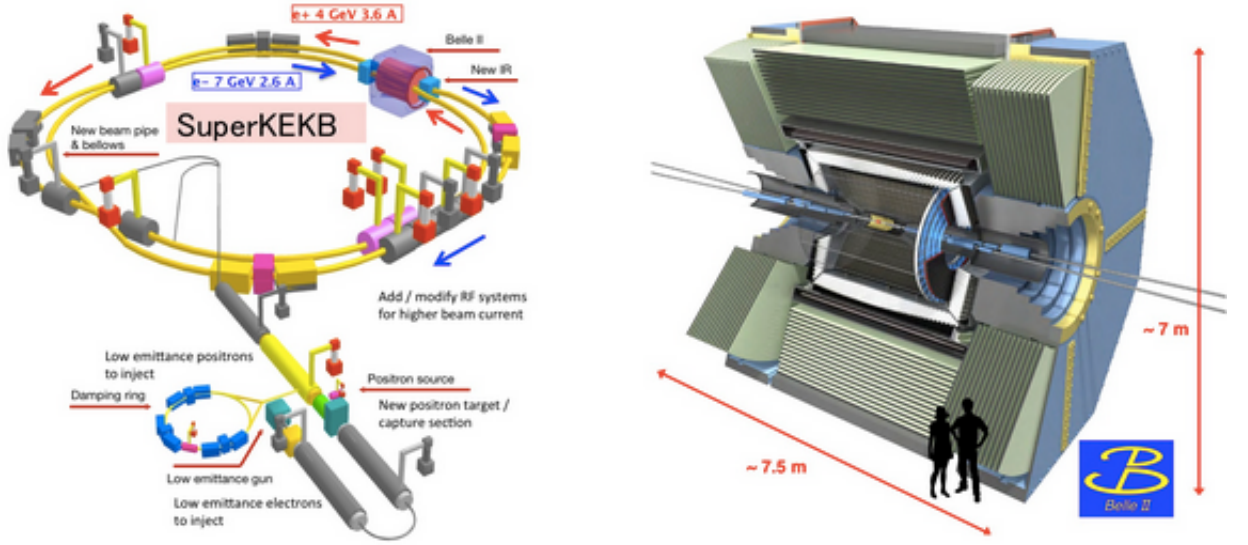


Figure 3: This is a schematic plot of SuperKEKB (left) and Belle-II detector(right).

gas as they travel. A number of electrons and ions produced move speedily near the sense wire. The sense wire senses the motion and creates a pulse signal. The signal is then sent to the data acquisition (DAQ) system.

The design of the Belle-II CDC does not change much from the original, because Belle's CDC has worked very well throughout the past decade. However, SuperKEKB will produce collisions at 40 times higher luminosity, so the new CDC must be able to work in conditions with 20 times higher background noise. By adding more sense wires, CDC group members believe the signal-to-noise ratio can be improved.

The CDC is a barrel structure around the beam pipes, and sits just outside a cylinder of the inner detector called silicon vertex detector (SVD). One big change in the baseline design is that the outer detector to the CDC, the particle identification detector (PID), will shrink



Figure 4: Belle-II logo.

in size by a factor of 3, owing to the new technology called time of propagation counter. Due to this and in order to maintain the Belle level of performance in a high luminosity environment, the number of wires in the Belle-II CDC are doubled. The CDC for Belle has 8,464 sense wires and 25,392 field wires. The upgraded CDC for Belle-II will have 14,336 sense wires and 42,240 field wires. Wire Conguration of the Belle CDC are shown in the Figure 7(a) and the Belle-II CDC are in the Figure 7(b). The filled circle shows an axial wire and the open circle shows a stereo wire.

One of the key issue is to balance weight of the wires, the wire tension, and the performance deterioration due to gravitational sag of the wires. Since wires are strung horizontally, gravity makes the sense wires sag at the middle. The sagging can affect measurements.

The sag due to gravitation for a range of tensions is calculated, and the effect on the performance is simulated by CDC group members. So far, the influence of sagging on the performance of the detector

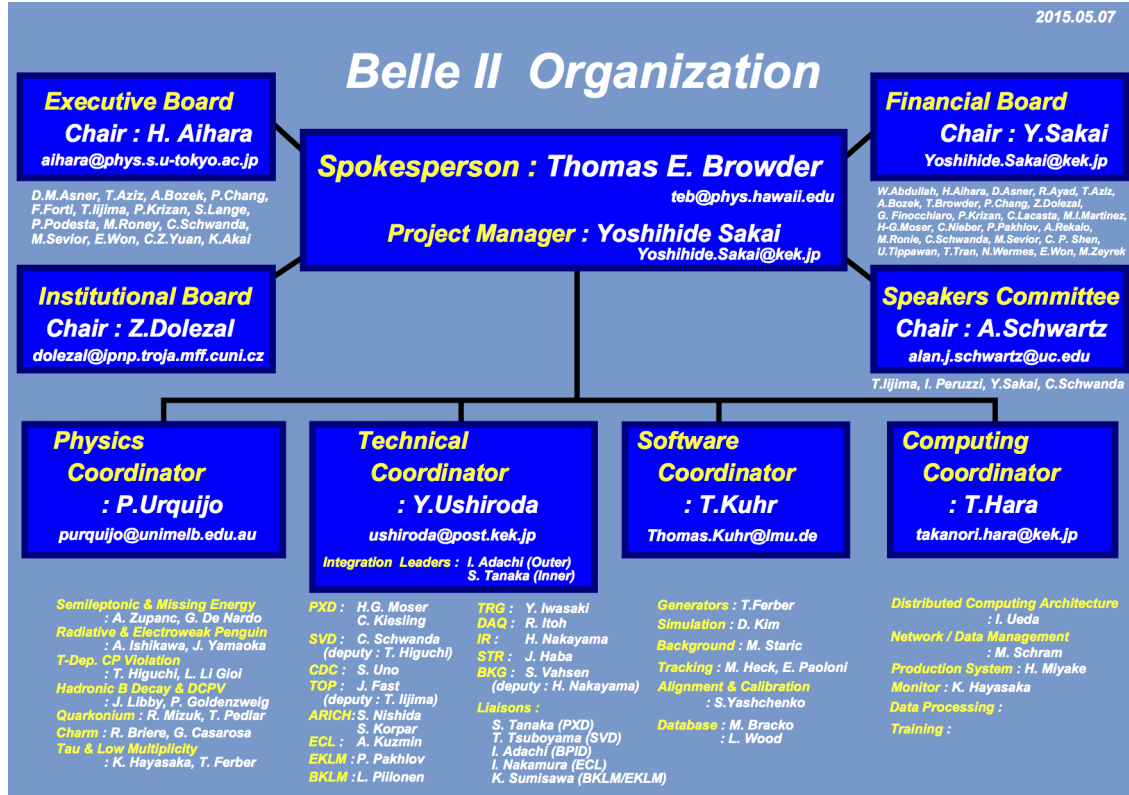


Figure 5: The Belle-II organization.

is smaller than the influence of the detector's inherent mechanical resolution.

The biggest concern, however, is the tension on the end plates due to the wires. The Belle CDC's thirty thousands wires produce 3 tons of force, displacing the location of the endplates as much as 3 millimeters. The Belle endplates are shaped so that particles entering the CDC have to go through minimum distance of material. The cross sectional view of the endplates are therefore curved so that particles from the interaction point would fly through no more than one centimeter of the endplate thickness in radial direction.

The endplates for the Belle-II CDC will have to endure 4 tons of

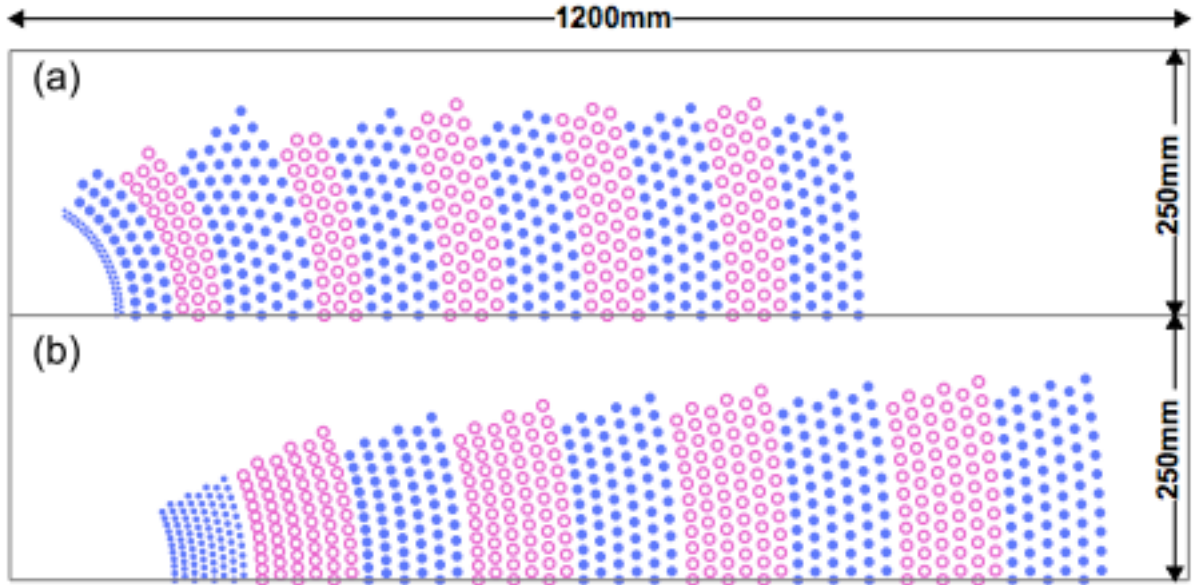


Figure 7: Wire Conguration of the Belle CDC (a) and the Belle-II CDC (b). The filled circle shows an axial wire and the open circle shows a stereo wire.

other, and of wires arranged in varying angles - called stereo wires. Six layers of axial wires make one group and six layers of stereo wires make another. The Belle-II's CDC has nine groups of these.

In addition, there will be eight layers of tightly spaced axial wires at the inner part of the CDC. This group is called a small cell. Past experience has shown that the introduction of a small cell in a chamber helps separate signals from noise by tracking particles freshly coming out of the interaction point.

0.3 The Readout Electronics of the CDC

The Belle CDC readout electronics will be completely replaced, owing to advancements in technology over the last two decades. The Belle-II CDC will employ an all-in-one technology that amplifies the signal,

applies a pulse shaping, and then converts the analog signal into a digital signal.

The Belle CDC sends signals all the way from the detector to an electronics hut 30 meters away via 30-meter cables to interpret the signals for data analysis. In the Belle-II CDC, all the electronics will be inside the Belle-II detector, right beside the chamber itself. Digitalized data will be readily available through fiber optic connections, to be collected in the DAQ system.

Signals from wire chamber is very small, so they are amplified by preamplifier component of the electronics. Amplified signals are shortened to make sure sensitivity to higher frequency signals in Belle-II. The electronics also need the ability to separate noise from signal. These functions, called shaping and discrimination, will be built into the new electronics. The electronics will use an application-specific integrated circuit (ASIC). An ASIC is a chip specially designed for a particular use. The new ASIC will process eight channels on a 4-millimeter by 4-millimeter chip for Belle-II, whereas the previous chip processed one channel on a 1-centimeter by 3-centimeter chip for Belle.

S. Uno said, ASIC technology was uncommon in Japan 20 years ago when CDC team were starting the design for Belle. Now that we have this technology, CDC team can develop custom chips for various projects. By using the technologies made available by KEK's Electronic System Group, CDC team can create compact, high-speed, and low power readout electronics.

N. Taniguchi successfully demonstrated the newly designed ASIC

electronic device in 2010. She also investigated optimal values for such parameters as gain, noise cancellation, and time resolution, using a hybrid board that contained all necessary parts.

Belle's CDC is already a good system. However, the system for Belle-II CDC is much more complex. A lot of the Belle-II CDC design is based on the past experience. Sometimes it's necessary to go beyond experience and make educated guesses in chamber science.

The Belle CDC uses bare aluminum for the field wires. Because aluminum cannot be soldered and is easily oxidized, no drift chamber had previously used bare aluminum. Other similar chambers have used gold-coated aluminum. For the Belle-II, however, CDC needs light wires. So aluminum wires are used without the gold coating. Since aluminum cannot be soldered to the endplates, the Belle-II CDC's wires are fixed by crimping pins. As to oxidation, S. Uno has found that aluminum oxidization does not affect the performance of the detector.

Before the B Factory experiment, most drift chambers were filled with an argon-based gas mixture. This was because argon is inexpensive, and also sensitive to X-rays. For initial testing of drift chambers, experimenters often used X-rays with an energy similar to the energy lost by the charged particles produced at the collider. For the B Factory, however, X-rays are considered as background noise. In addition, because argon is so heavy, it can destruct the momentum measurement of particles. To solve this problem, the CDC team developed an X-ray insensitive, light gas mixture consisting of helium and ethane.

Drift chambers are packed with the very basics of particle physics experiment, and cultivate creativity and good intuitions. In Taiwan, four High Energy experimental research groups are encouraged to join this CDC team. They are National Taiwan University (NTU), National United University (NUU), National Central University (NCU) and Fu Jen Catholic University (FJU).

I am a team member in FJU and my advisor is Jeri M.C. Chang. We FJU team is highly cooperated with Y. Iwasaki-san at KEK. My master thesis is mainly for my tasks done in 2D tracker simulation design at CDC Level 1 Trigger system. My classmate Z.X. Chen works closely with me and his tasks is mainly for 2D tracker firmware (VHDL). In my thesis, I will use some of his studies to explain my decision making in simulation algorithm. The firmware testing details are in his thesis. Z.X. Chen and I work together with the content of this chapter, so we share the same content in our chapter 1 in the thesis.

Chapter 1

The CDC Trigger System

1.1 Introduction

The CDC plays an important roles for providing trigger signal and reconstructing charged track.

The Belle CDC has been operated well for more than ten years. In the case of Belle-II experiment, the CDC changes the design. The super-layer configuration and the cell structure are modified.

The CDC uses many sense wires and field wires for detecting triggered signals.

There are nine super layers in the CDC. Each super layers have six layers, the even super layers 0, 2, 4, 6, 8 are axial layers, which are used for 2-D tracker. For the odd layers 1, 3, 5, 7 are stereo layers, which are used for 3-D tracker. In the Figure 1.2, it is a simple schematic top view of the locations of super layers. Main parameters of the Belle CDC and the Belle-II CDC are listed in the Figure 1.1.

	Belle	Belle-II
Radius of inner boundary (mm)	77	160
Radius of outer boundary (mm)	880	1130
Radius of inner most sense wire (mm)	88	168
Radius of outer most sense wire (mm)	863	1111.4
Number of layers	50	56
Number of total sense wires	8400	14336

Figure 1.1: It is the parameter of CDC between Belle and Belle-II.

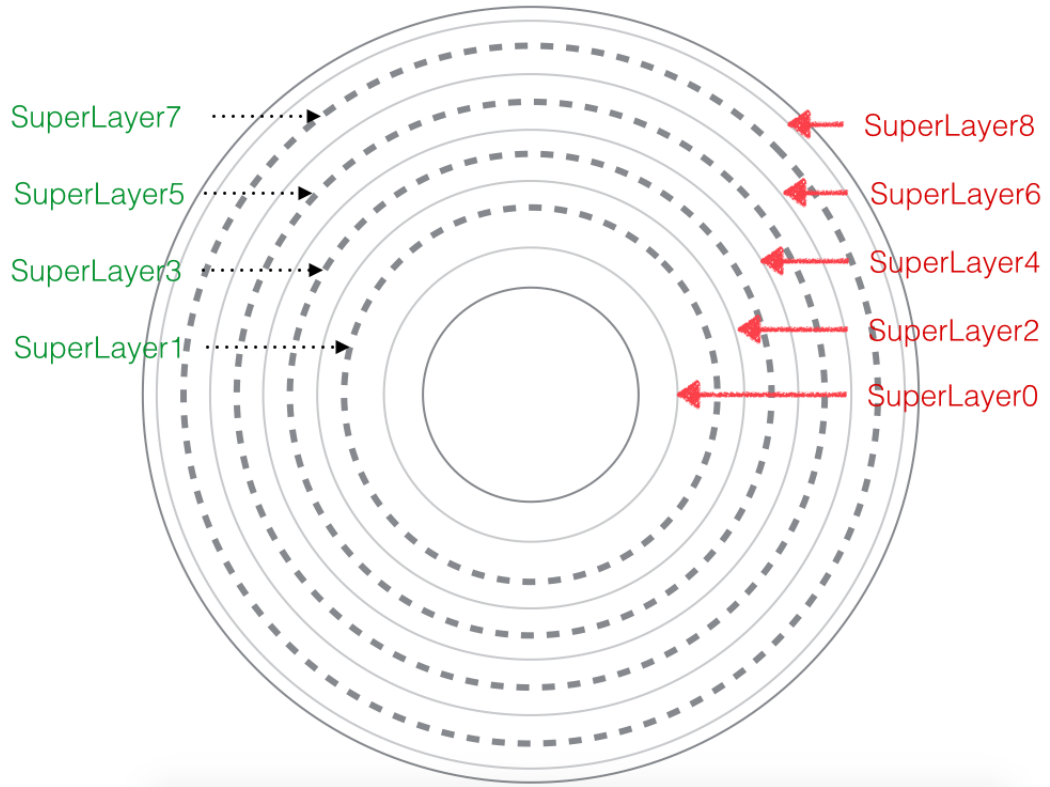


Figure 1.2: It is a simple CDC schematic top view of the locations of super layers.

1.2 The Front-end and the Merger

Belle-II detector signals are digitized in an internal front-end electronics card (CDC, TOP, and ARICH) or nearby (SVD, ECL, and KLM) the detector. The digitized signals, except for the PXD, are collected by FPGAs on front-end electronics cards. There are approximately 15,000 CDC readout channels. Because of mechanical constraints, the size of each CDC front-end electronics cards is $20 \times 17 \text{ cm}^2$ for 48 channels.

Since the front-end electronics of the CDC, TOP, and ARICH are located inside the detector, the effects of radiation on their components will be a severe problem. The expected annual neutron flux and γ -ray dose from the beam background at the CDC innermost layer is about $\sim 10^{11}/\text{cm}^2$ and $\sim 30 \text{ Gy}$, respectively, at design luminosity.

Each of 48 CDC sense wires are connected to front-end board. A multiplexer in the front-end board can generate the discriminated signals in each pulse by using a 1 GHz clock. These precise wire-hit signals are down-sampled by a 62.5 MHz clock. One-bit hit from the 48 CDC sense wires on the front-end board is sent to the merger multiplexer by the high speed serial links.

The merger multiplexer receives 6 wire layers information from the front-end board, and merges the 6 layers information to 5 layers. The 5 layers information will be sent to TSF module.

The schematic of the Front-End and Merger are shown in the Figure 1.3 and in the Figure 1.4, respectively.

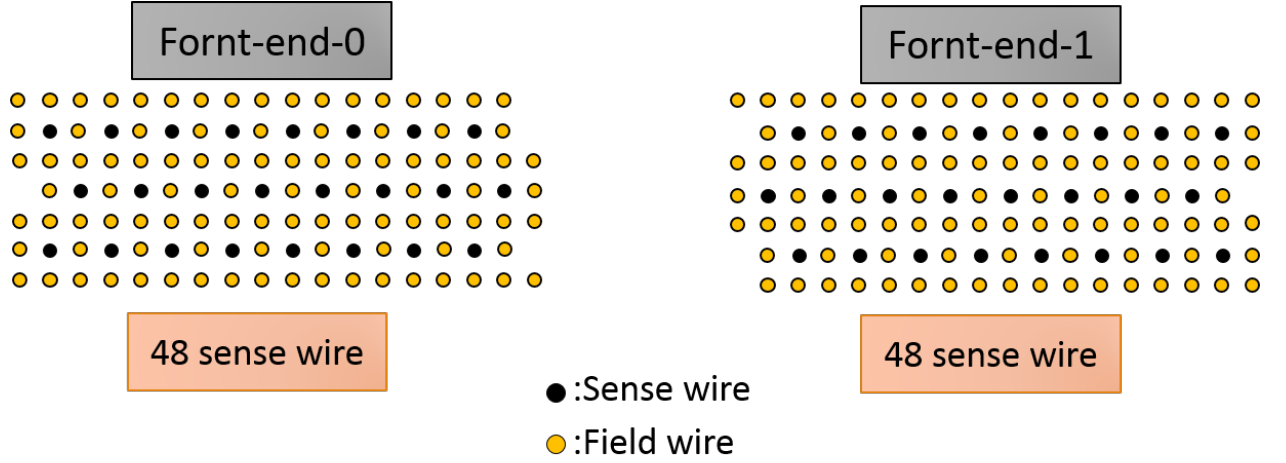


Figure 1.3: Schematic of the Front-End structure

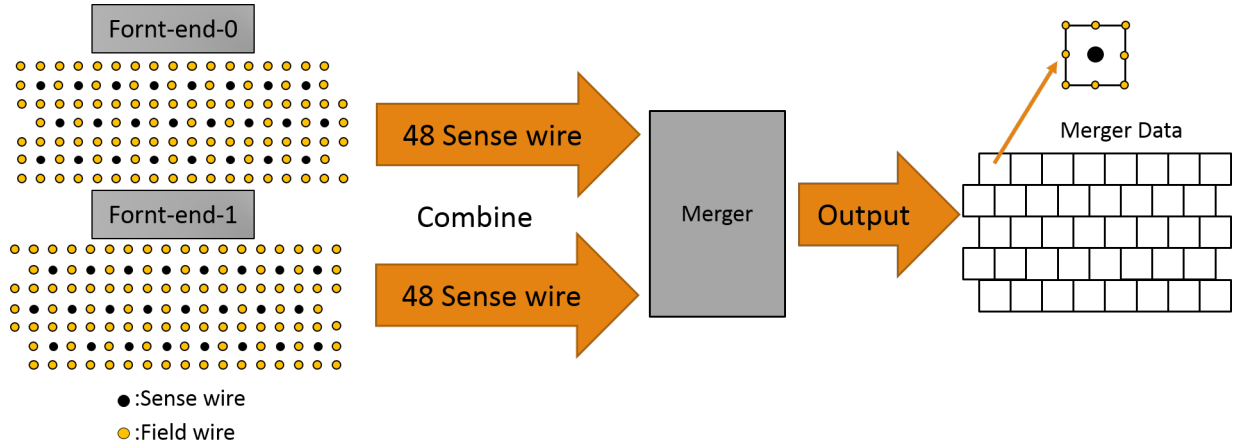


Figure 1.4: Schematic of the Merger structure.

1.3 The Track Segment Finder (TSF)

The wire-hit information collecting from the Merger, is sent to the Track Segment Finder (TSF). The TSF uses one Universal Trigger Board (UT3) per super-layers. There are 9 super-layers in total. So, nine UT3 are used for TSF module as well.

There are 11 Track Segments (TS) combined as one Track Segment Finder (TSF). Each TS consists 8 Field wires in the outside box and 1 Sense wire in the center. The sandglass shape is the normal shape of TSF. For the TSF shape in the innermost superlayer, their shape is triangle. The TSF will be triggered only if there are more than 1 hit in each TS layer. But, in case of the broken sense wires, we also allow 4 layer hit TSF be triggered.

The TSF module will send the triggered signals in axial super layers and the hit patterns to 2D tracker module. For 3D tracker module, TSF will send the triggered signals in stereo super layers and the hit patterns at the same time. The hit pattern means the algorithm in the TSF will adjust the hit tendency as right, left, or unknown. The hit information means the serial number of hitted wires. By knowing this wire hit information, the 2D and 3D tracker can do the track analysis.

CDC Trigger also have event timing module (EVT) to provide timing information for 2D and 3D tracker modules as well. This EVT module is important for 2D and 3D tracker modules. Because knowing the drift time, we can know the exactly hit range in each layer and obtain the best track resolution by fitting.

1.4 The 2D and 3D tracker

The 2D and 3D tracker module use the Universal Trigger Board (UT3). By modifying the firmware inside the FPGA chip, we can change the performance of the UT3 as 2D and 3D tracker module.

The 2D tracker module is made for determining the trajectory in

the CDC x-y plane. The 3D tracker module is made for determining the trajectory in the CDC x-y-z plane. Because of the hardware constraints, we need to finish 2D trajectory first and sent the information to 3D. In case of comparing the resolution of 2D and 3D tracker module, both of these modules will send trajectory information to Belle-II Global Decision Logic (GDL). The GDL is the central computer system for collecting level 1 trigger signals from each sub-detectors. The following data analysis will take place after receiving trigger signals.

Chapter 2

The Hough Voting for 2D Tracker

2.1 Hough Transform

The Hough transform is a feature extraction technique used in image analysis. The purpose of the technique is to find imperfect instances of objects within a certain class of shapes by a voting procedure [6].

2.2 Circle Hough Transform

Each point in 2 dimensional space (x-y plane), we can find two kinds of circle that will pass through the origin point $(0,0)$ and the point itself. One kind is called right-handed circle, and the other is called left-handed circle. A simple plot for the two kinds of circles is shown in the Figure 2.1.

In order to explain the circles in formula, we use the equation (2.1). Here x and y are the coordinate variables. The a and b are the parameters for center of the circle. The r is the radius of the circle.

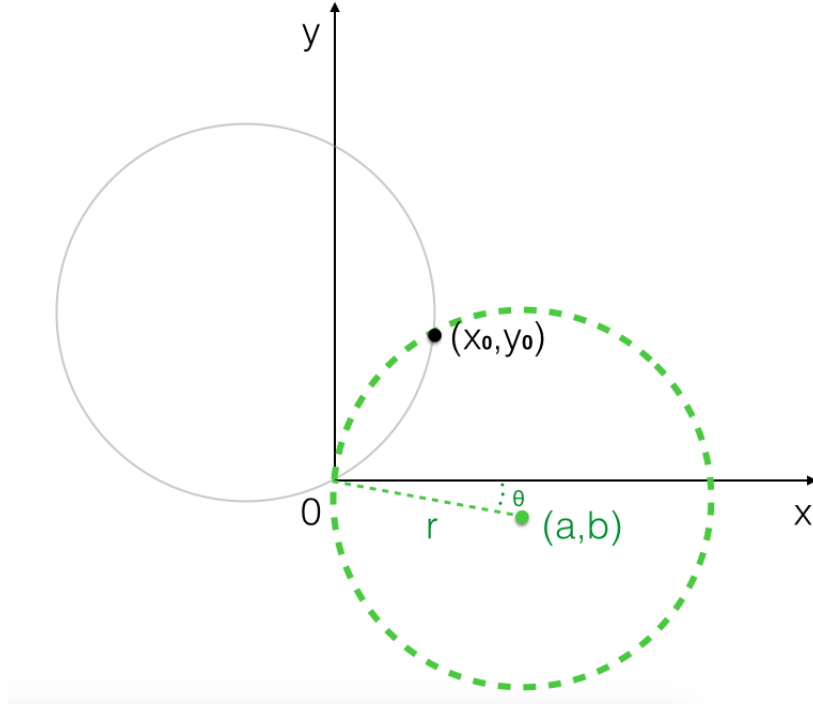


Figure 2.1: Schematic view of the right handed and left handed circles in the CDC x-y plane. The dashed circle is named right-handed circle and the solid circle is named left-handed circle.

$$(x - a)^2 + (y - b)^2 = r^2 = a^2 + b^2 \quad (2.1)$$

By expanding the equation (2.1), we obtain the equation as equation (2.2).

$$x^2 - 2ax + y^2 - 2by = 0 \quad (2.2)$$

Then, we replace the a and b parameters from the x, y coordinate into polar coordinate. We use equations (2.3) and (2.4). The r is the radius and ϕ is the polar angle of the circle.

$$a = r \cos \phi \quad (2.3)$$

$$b = r \sin \phi \quad (2.4)$$

By replacing the a and b variables in the equation (2.3) and (2.4) to (2.2). Then we have the equation as (2.5).

$$x^2 - 2xr \cos \phi + y^2 - 2yr \sin \phi = 0 \quad (2.5)$$

We rewrite the equation (2.5) into the equation (2.6).

$$r = \frac{x^2 + y^2}{2x \cos \phi + 2y \sin \phi} \quad (2.6)$$

If we put a known point (x_0, y_0) into the equation (2.6), we can obtain the equation (2.6) again as in the equation (2.7).

$$r = \frac{x_0^2 + y_0^2}{2x_0 \cos \phi + 2y_0 \sin \phi} \quad (2.7)$$

The two variables r and ϕ in the equation (2.7) are the basis of the Hough plane. I use $\log(r)$ and ϕ as the Hough plane basis for a better scale size. The $\log(r)$ range is between 1.824 to 3.204 and ϕ is 0 to 2π .

In the Figure 2.2, it shows a point (x_0, y_0) corresponding to two arcs which fits the condition in the equation (2.7).

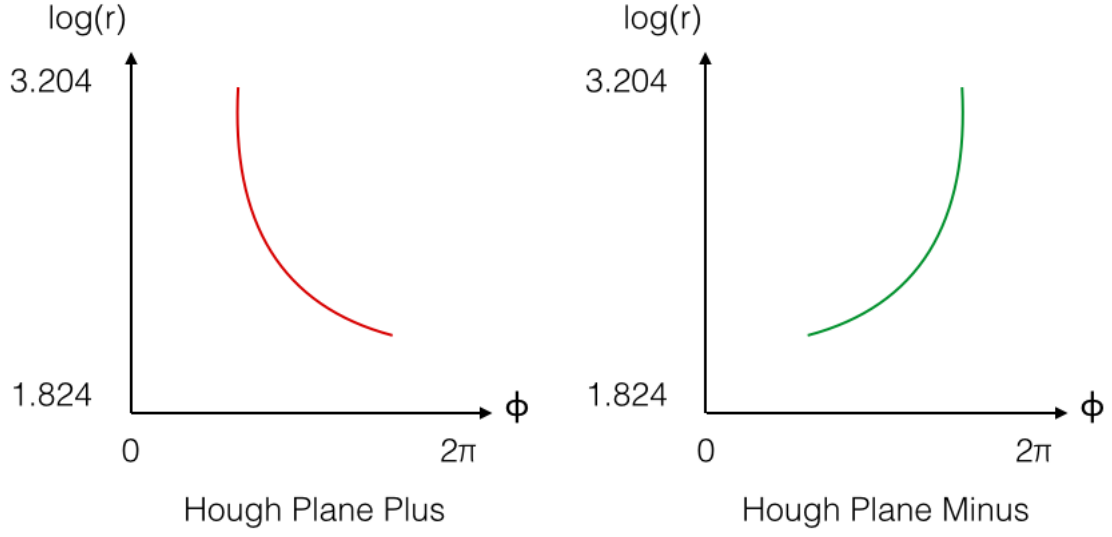


Figure 2.2: A point (x_0, y_0) corresponding to two arcs which fits the condition in the equation (2.7).

We separate the arcs into two planes. One plane is called Hough Plus plane, and the other is called Hough Minus plane. Their names indicate their charge: positive or negative charge tracks.

In the 2d tracker study, we literally collect the wire hits from the 5 even super layers. If there are 5 wire hits (as shown in the Figure 2.3) which can be turned into 5 arcs in the Hough Plus plane and 5 arcs in the Hough Minus plane (as shown in the Figure 2.4). The intersection point in the Hough plane means that 5 points are in the same track circle (as shown in the Figure 2.5).

2.3 Arcs to mesh

Ideally, the arcs in Hough plane should be perfect curves. But it would be impossible for the software calculations. So, I slice the Hough plane.

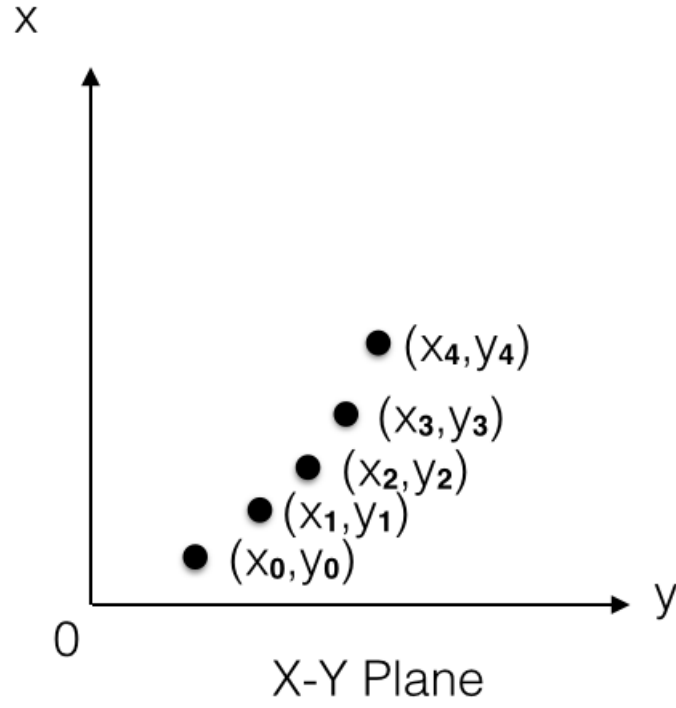


Figure 2.3: Five wire hits in x-y plane.

I slice sections into 160 in the ϕ axis and 16 in the $\log(r)$ axis. A plot in the Figure 2.6 shows the idea of transforming the arcs into meshes. An example of transforming the arcs into meshes in TSIM is shown in the Figure 2.7.

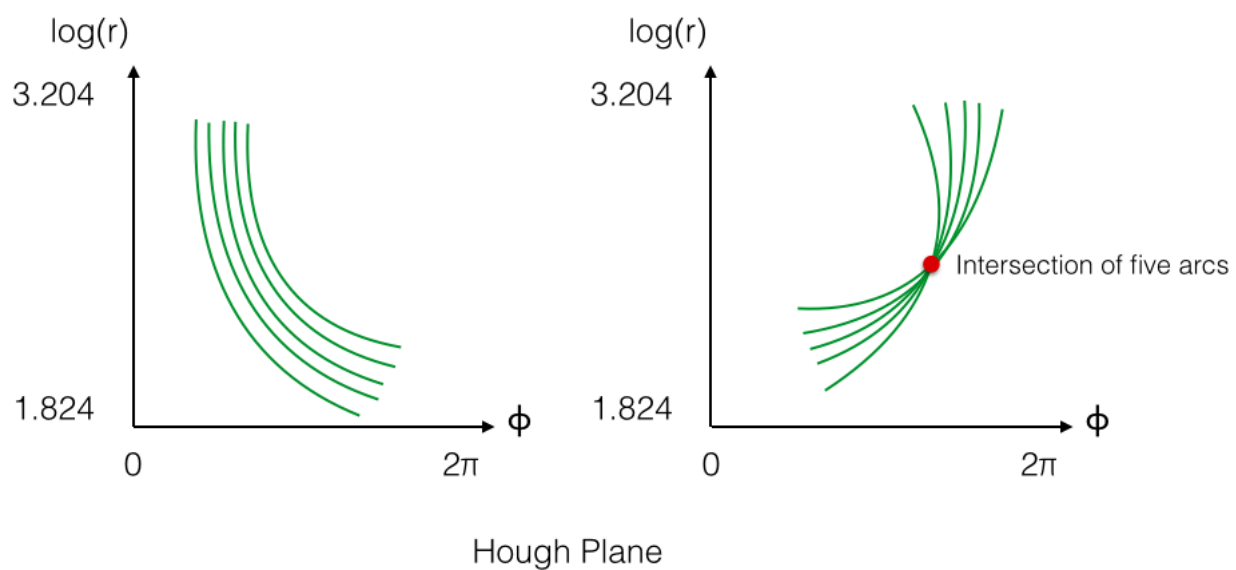


Figure 2.4: Five arcs in Hough Plus and Minus plane.

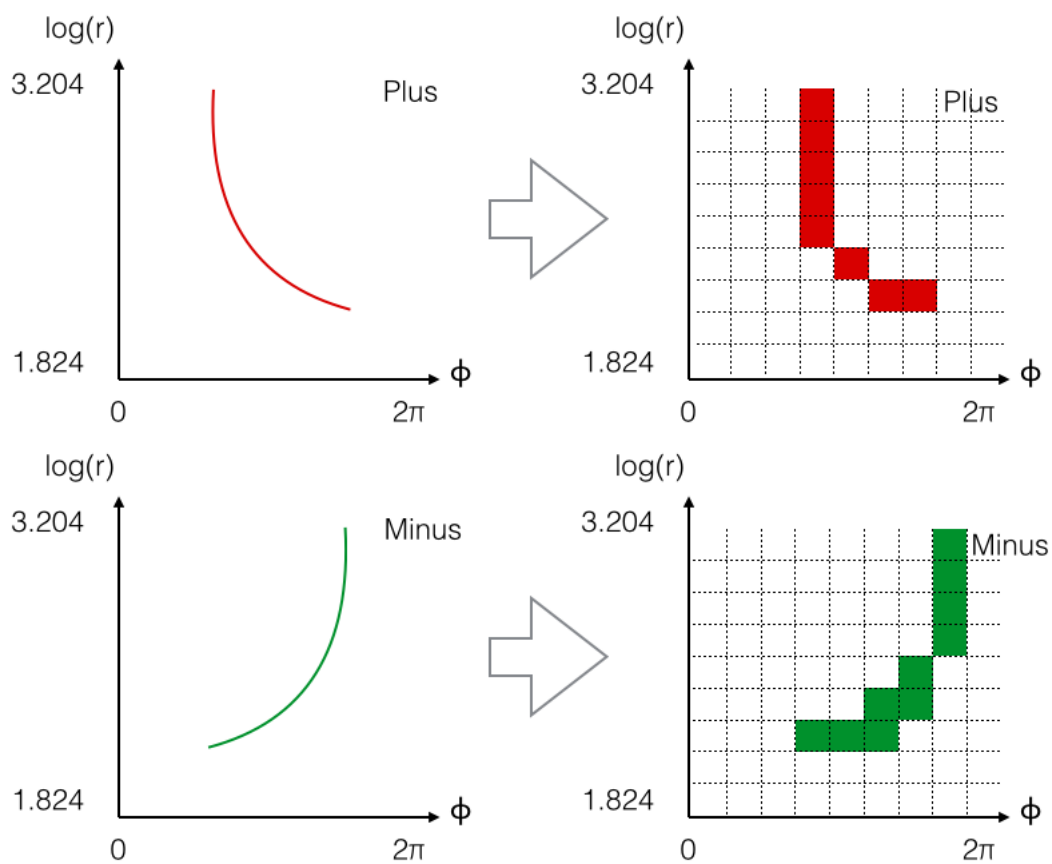


Figure 2.6: The idea of transforming the arcs into meshes.

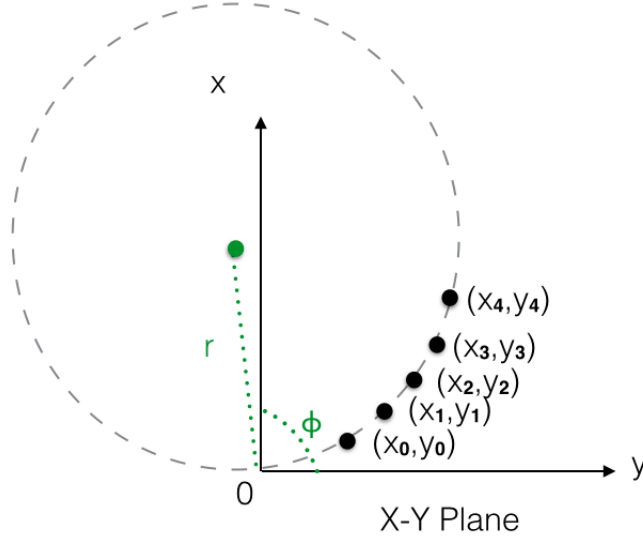


Figure 2.5: The cross point in the Hough plane means that 5 points are in the same track circle.

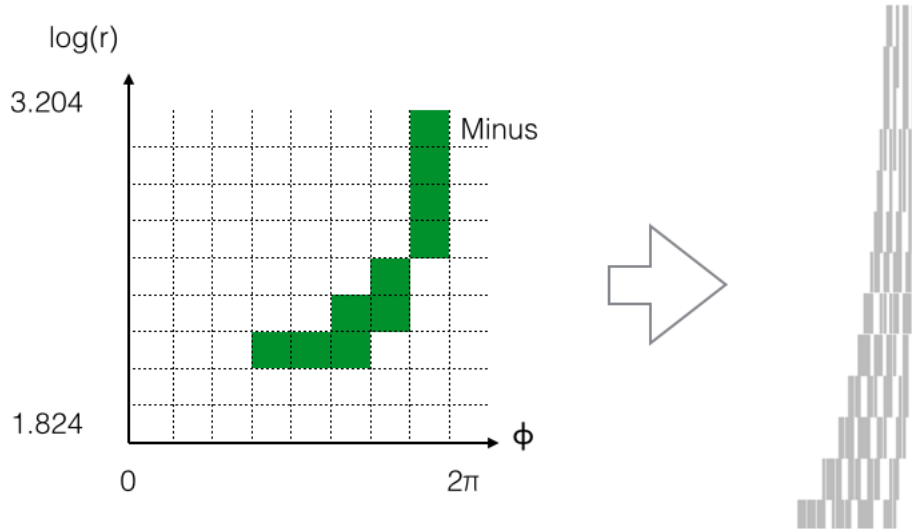


Figure 2.7: An example of transforming the arcs into meshes in TSIM.

To know the relation between TSF and the Hough cells in advance, we can connect those TSFs to trigger the Hough cells. We use OR logic for the relationship between Hough cells and TSFs.

After we have the TSFs connected to Hough cells, we can connect the Hough cells in the same position in each super layer. We use AND logic for this superposition. The idea is shown in the Figure 2.8. What we obtained is the five hits Hough cells in the Hough voting process.

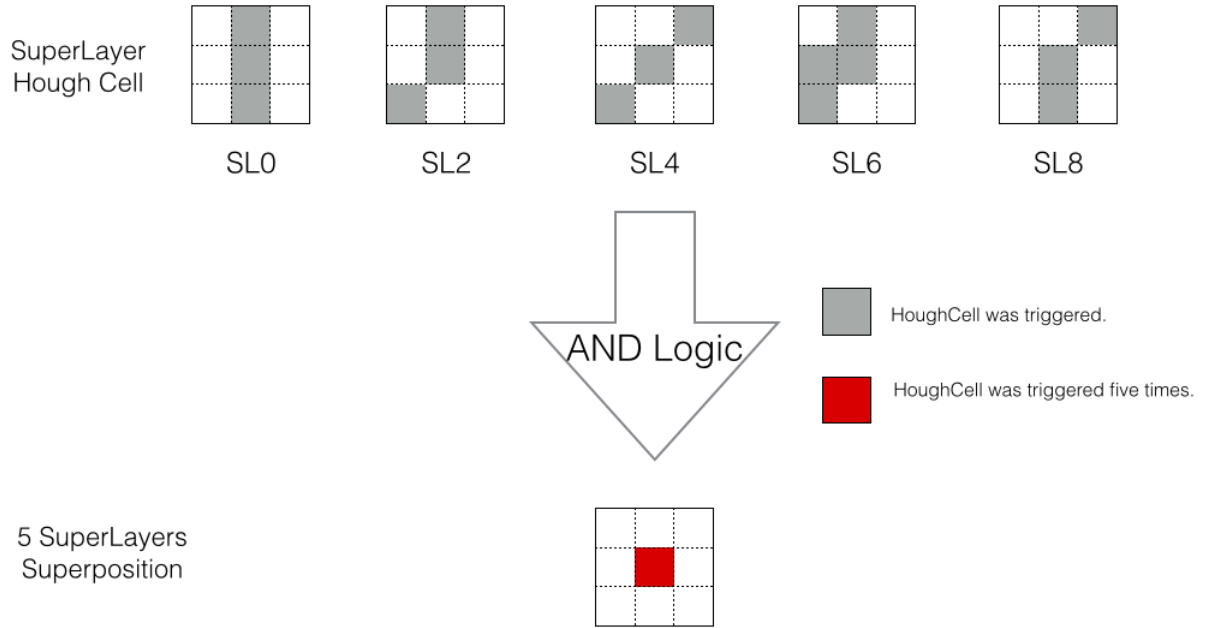


Figure 2.8: After we have the TSFs connected to Hough cells, we can connect the Hough cells in the same position in each super layer. We use AND logic for this superposition.

Chapter 3

The Peak Finding for 2D Full and Short Tracker

The peak finding is a method to find the cluster center among those connected hit cells in the Hough plane.

3.1 Hough Cell Clusters

In the Hough Plane, we can have connected hit cells as shown in the Figure 3.1. The connected cells are called clusters.

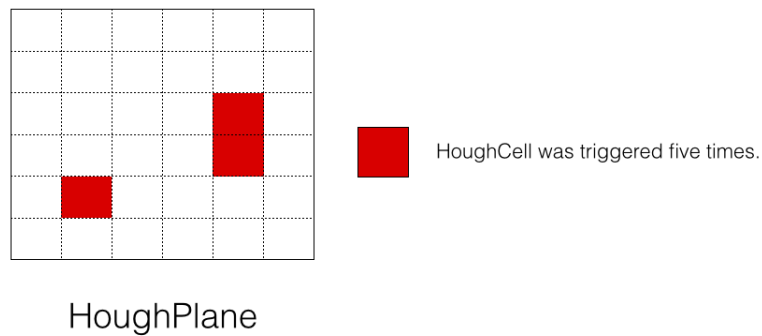


Figure 3.1: The connected hit cells in the Hough Plane are called clusters. In this plot, there are two clusters.

3.2 Finding the Regions

To obtain the regions(or number of clusters), we can not count them by eyes. I have five steps for counting them.

- Step 1 The hit cells are scanned from the left to the right, and from the bottom to the top. If there is a cell triggered for five times, then go to Step 2. Otherwise the process will go to step 5.
- Step 2 The process will set the five hit cell as the center cell, and then go to Step 3.
- Step 3 The process searches for the neighbors of the center cell.

The neighbor searching for Hough Minus plane should be only in the right, upper right, up and upper left. But, for the Hough Plus plane, its neighbor searching should be only in the left, upper left, up and upper right. In the Figure 3.2 and Figure 3.3, they show the searching range and the cluster combined process.

- Step 4 After Step 3, if the center cell has neighbor cells, these cells will be labelled as the same cluster number (region). If not, go back to step 1.
- Step 5 Stop scanning.

The Figure 3.4 is an example of the results after clustering.

Some tracks are very close to each other, an example is shown in the Figure 3.5. In order to solve this kind of very close track problem, we study the neighbor relation again. Because the segment in ϕ direction

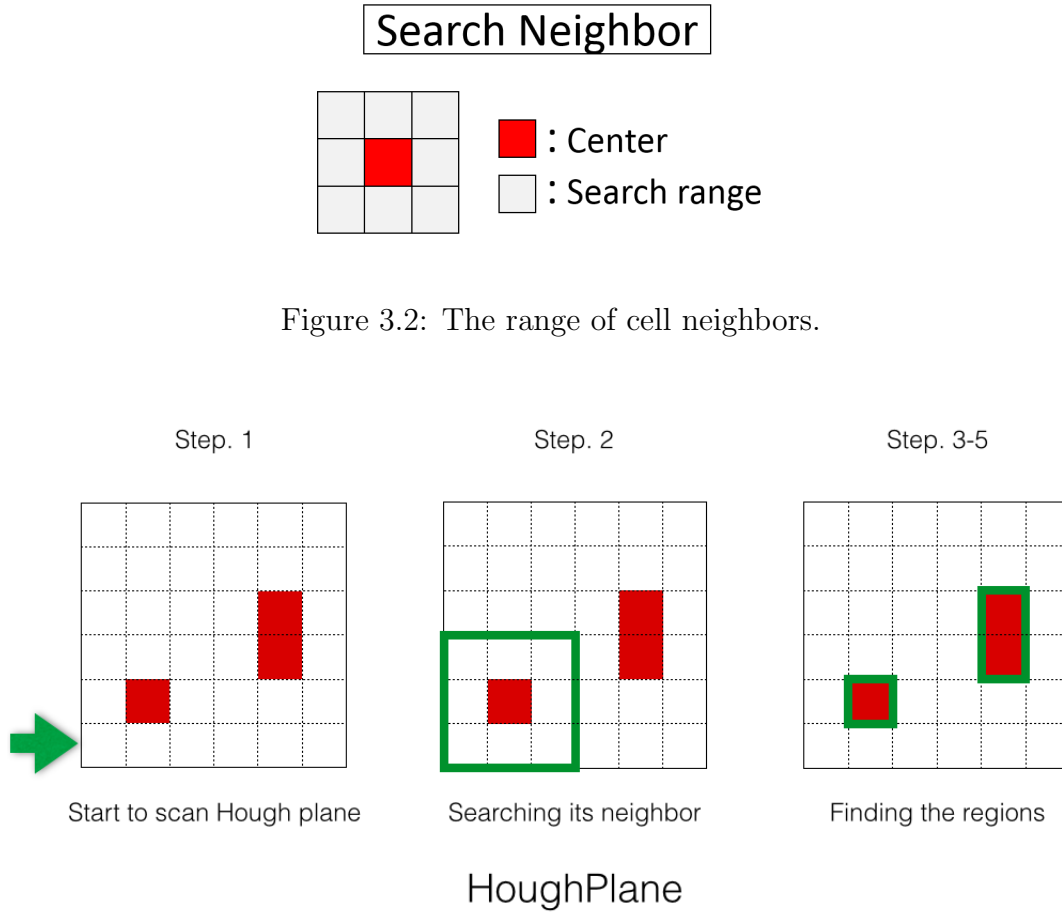


Figure 3.3: Searching process of clusters.

could be too small, we extend the definition of neighbor. We allow the neighbor cells are within a 2×3 region. Two allowed neighbor cases are shown in the Figure 3.6.

We update the neighbor scanning region as shown in the Figure 3.7. After this modification, the very-close-tracks problem is much reduced in TSIM. In the Figure 3.8, it shows the difference between previous cluster neighboring and updated neighboring. The very close tracks are combined as the same cluster.

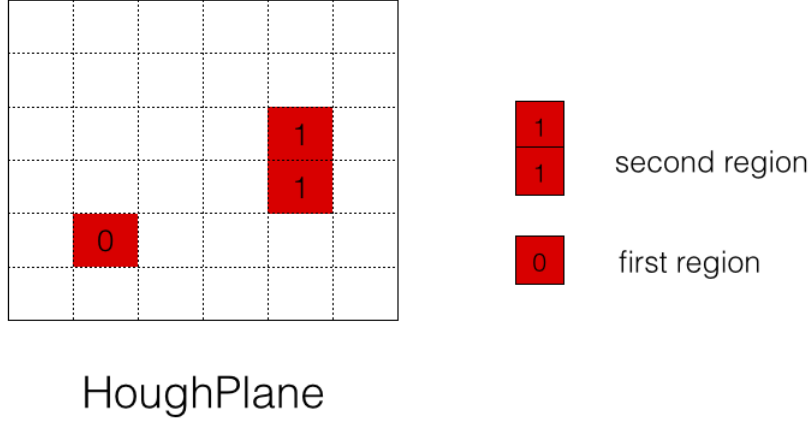


Figure 3.4: An example of the results after clustering.

3.3 Center of Cluster

We follow the steps below to find the center of each cluster.

- Step 1 Go to the Regions function and select one of regions(or clusters). Scanning process is from Region 0, 1, ... to the end.
- Step 2 Calculate the center of the cluster. We average the positions among the hit cells. The calculation function is as below.

$$\left(\frac{\max \phi + \min \phi}{2}, \frac{\max \log(r) + \min \log(r)}{2} \right)$$

In TSIM, this type of center cell is in integral. If the center position is not an integer, the numbers below 1 will be given up. Calculate the distance between the center and each cells.

- Step 3 The cell closest to the center will be identify as the cell center. If there are more than 1 candidate, we will select the first scanned cell as the cell center.

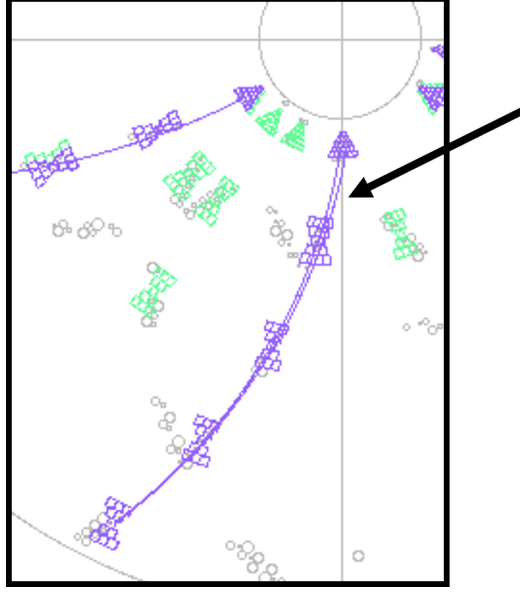


Figure 3.5: Some tracks are very close to each other, an example is shown here.

- Step 4 The final cluster center is the selected cell center.

3.4 Mesh Size

The basic mesh size setting is $(r, \phi) = (180, 16)$. We change it to $(r, \phi) = (160, 16)$ because the superlayer0 has 160 TSs, we can get better accuracy and precision in the beginning of peakfinding.

After optimize the mesh size, the Hough Plane looks like the Figure 3.9.

Hough Plane

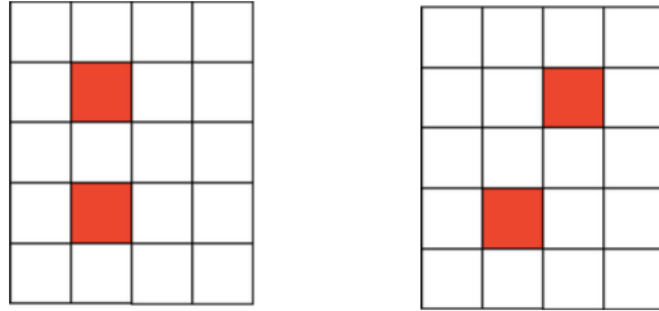


Figure 3.6: We allow the neighbor cells are within a 2 by 3 region. Two allowed neighbor cases are shown here.

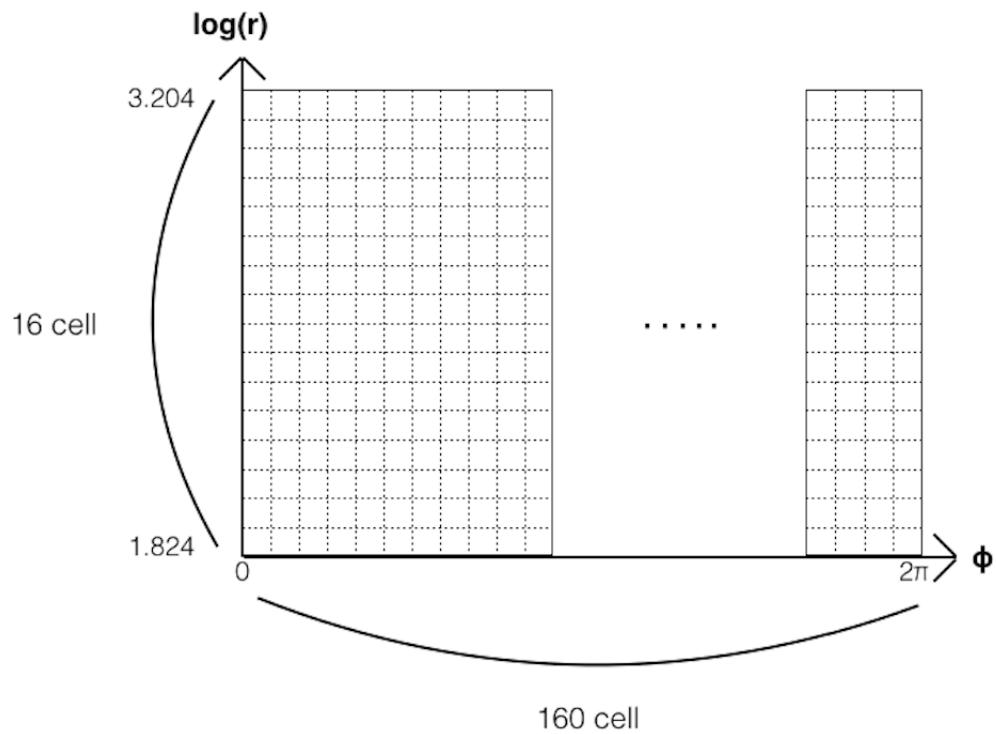


Figure 3.9: The dashed line means the cutting line that we remove the events below that line. In the Hough Plane, the lower 10 rows are removed.

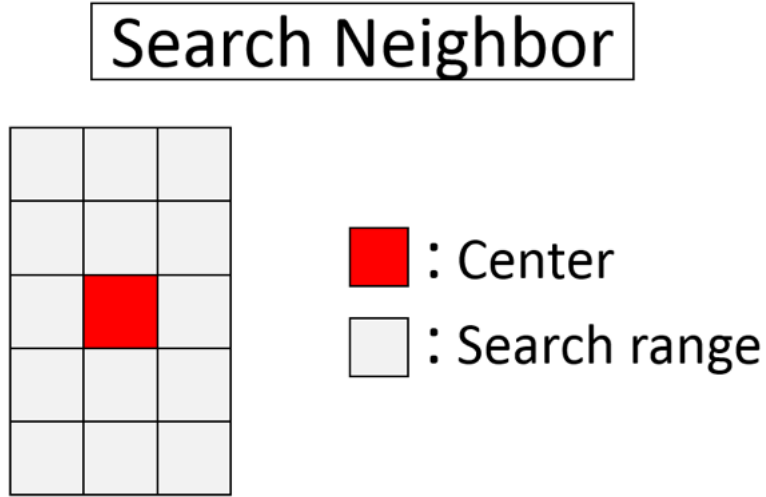


Figure 3.7: We update the neighbor scanning region to solve the very-close-tracks problem.

3.5 FPGA Algorithm

We use a method to reach the Hough voting and Peak Finding in the FPGA. For Hough Voting, we calculate the corresponding relation between Hough cell and the TSFs in advance. Then, we can easily connect the TSFs to Hough cells. We use OR logic for Hough Plane transforming and use AND logic for superposition of all Hough Plane in the even superlayers.

For the clustering, we use the method called Pattern I, Pattern II to find clusters. We decide the center of Pattern II and then Pattern I after finding the clusters,

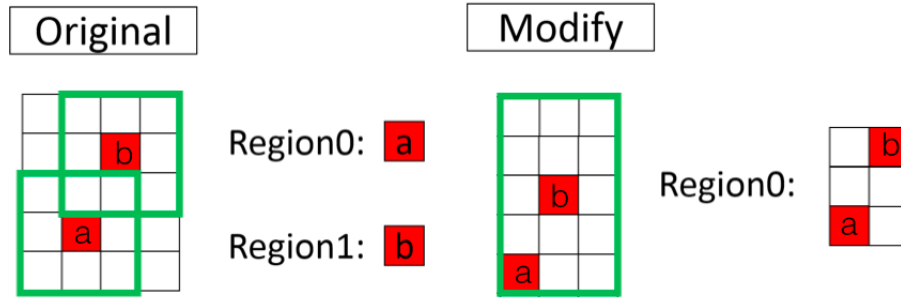


Figure 3.8: Here shows the difference between previous cluster neighboring and updated neighboring. In the updated case, the very-close-tracks problem is much reduced.

3.6 The relation among Pattern I

The Pattern I is a $2 \times 2 = 4$ cells, as described in the Figure 3.10. The four cells of Pattern I, they are labelled as a, b, c and d.

In the Hough plane, we have $160 \times 16 = 2560$ cells. This also means that we have $2560/4 = 640$ Pattern I. To have a overall look in the Hough plane, please check the Figure 3.11.

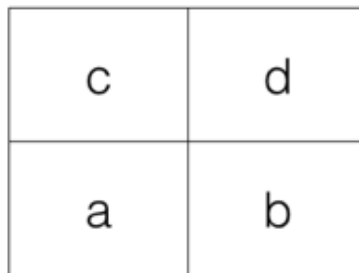


Figure 3.10: A Pattern I

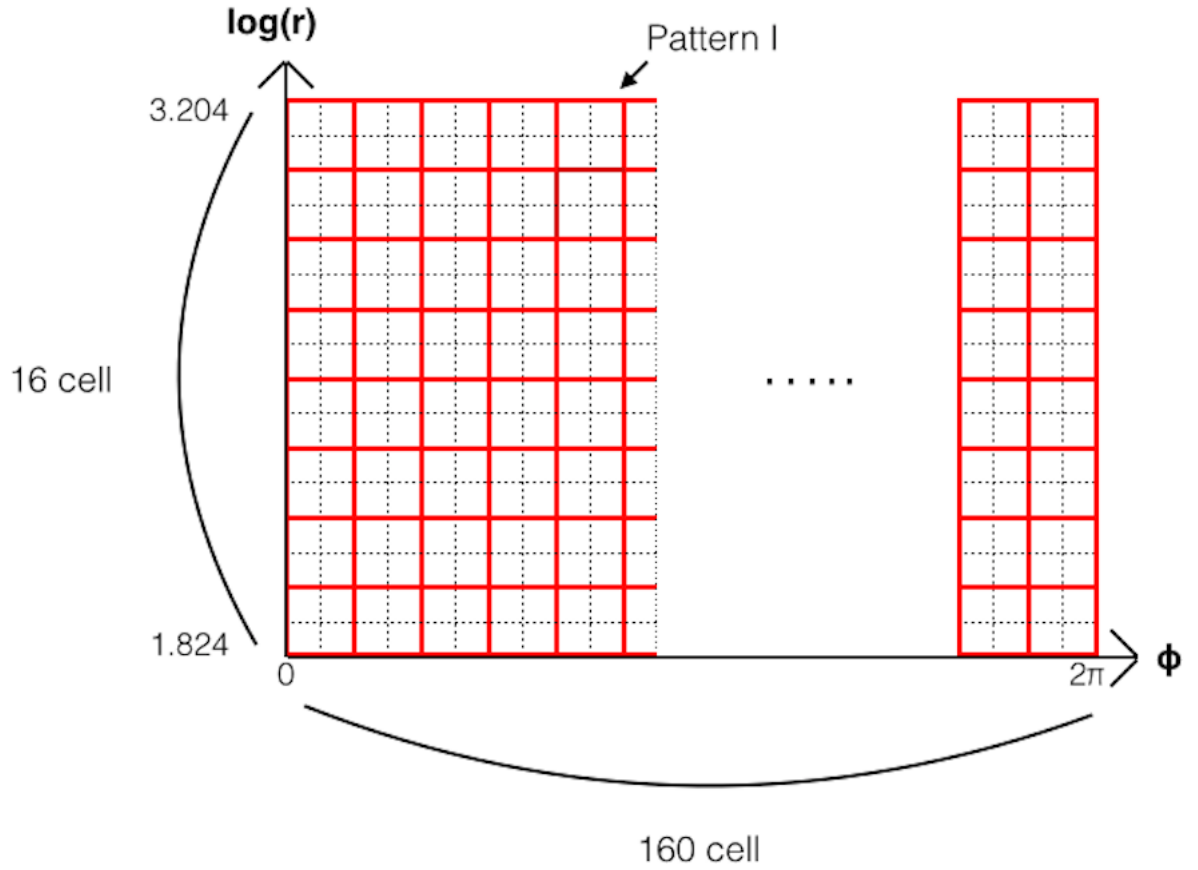


Figure 3.11: The relation between Pattern I and Hough plane.

3.7 The relation among Pattern II

The Pattern I is the basis of the Pattern II. A 3×3 Pattern I builds up a Pattern II. The Figure 3.12 shows a Pattern II, which consists the labelled A, B, C, D, E, F, G, H, and I part. The labelled X, Y, and Z means the neighbors of A part.

The Pattern II is the assumed maximum size of cluster.

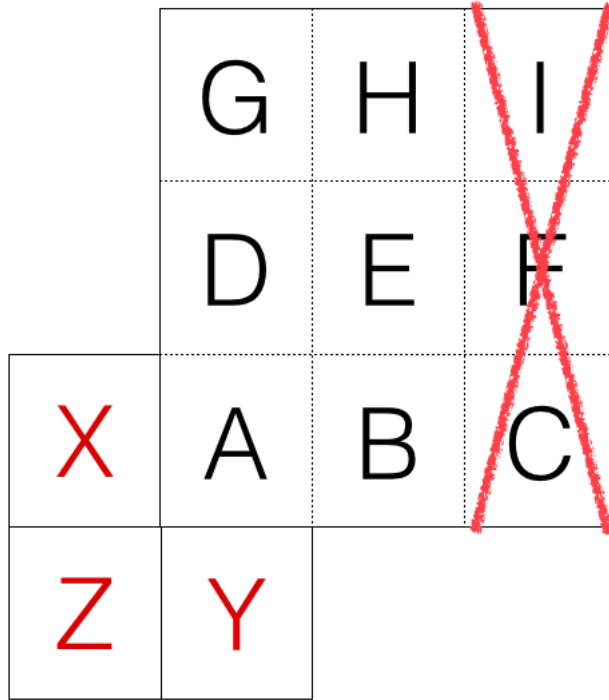


Figure 3.12: Because the outmost Pattern I(C, F, and I positions) in the setting obtains less than 1% hit rate, we make the cluster unit smaller..

The hitted rate of C, F, and I in the Pattern II. I found the hitted rate in the C, F, and I in the Pattern II is lower than 1%, as shown in the Figure 3.13. Because of this result, the Pattern II size becomes 2×3 in the 2D logic.

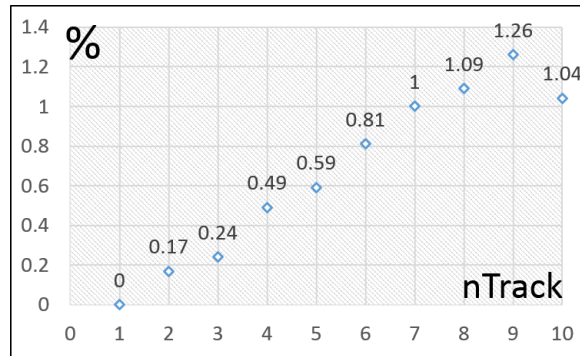


Figure 3.13: The hitted rate in the C, F, and I in the Pattern II

We follow the following seven steps to get the clusters.

- Step 1 Scan Pattern I from the left to the right, and from the bottom to the top. If a Pattern I is triggered, this Pattern I will be treated as the position A part.
- Step 2 If the neighbors of this Pattern A (X, Y, and Z) are triggered, then the relation between (A and X), (A and Y), and (A and Z) are compared. If one of them has relationship, then this Pattern II will be given up.
- Step 3 Compare the relation between (A and B). If (A and B) are related, the B triggered part are kept. Otherwise, the B triggered part are removed. Compare the relation between (A and D). If (A and D) are related, the D triggered part are kept. Otherwise, the D triggered part are removed. Compare the relation between (A and E). If (A and E) are related, the E triggered part are kept. Otherwise, the E triggered part are removed.
- Step 4 Compare the relation between (B and E). If (B and E) are related, the E triggered part are kept. Otherwise, the E triggered part are removed.

Compare the relation between (D and E). If (D and E) are related, the E triggered part are kept. Otherwise, the E triggered part are removed. Compare the relation between (D and G). If (D and G) are related, the G triggered part are kept. Otherwise, the G triggered part are removed. Compare the relation between (D

and H). If (D and H) are related, the H triggered part are kept. Otherwise, the H triggered part are removed.

- Step 5 Compare the relation between (E and H). If (E and H) are related, the H triggered part are kept. Otherwise, the H triggered part are removed.
- Step 6 For E, H part, they are checked the relations more than once. In their cases, any of them are related with the checked part, their triggered part are kept.

The relation comparsion between each Pattern I is described in the Figure 3.14. It is easier to check the non-related case so we use this skill to decide our look-up-tables. After the six steps, the PatternII becomes a cluster containing only one cluster.

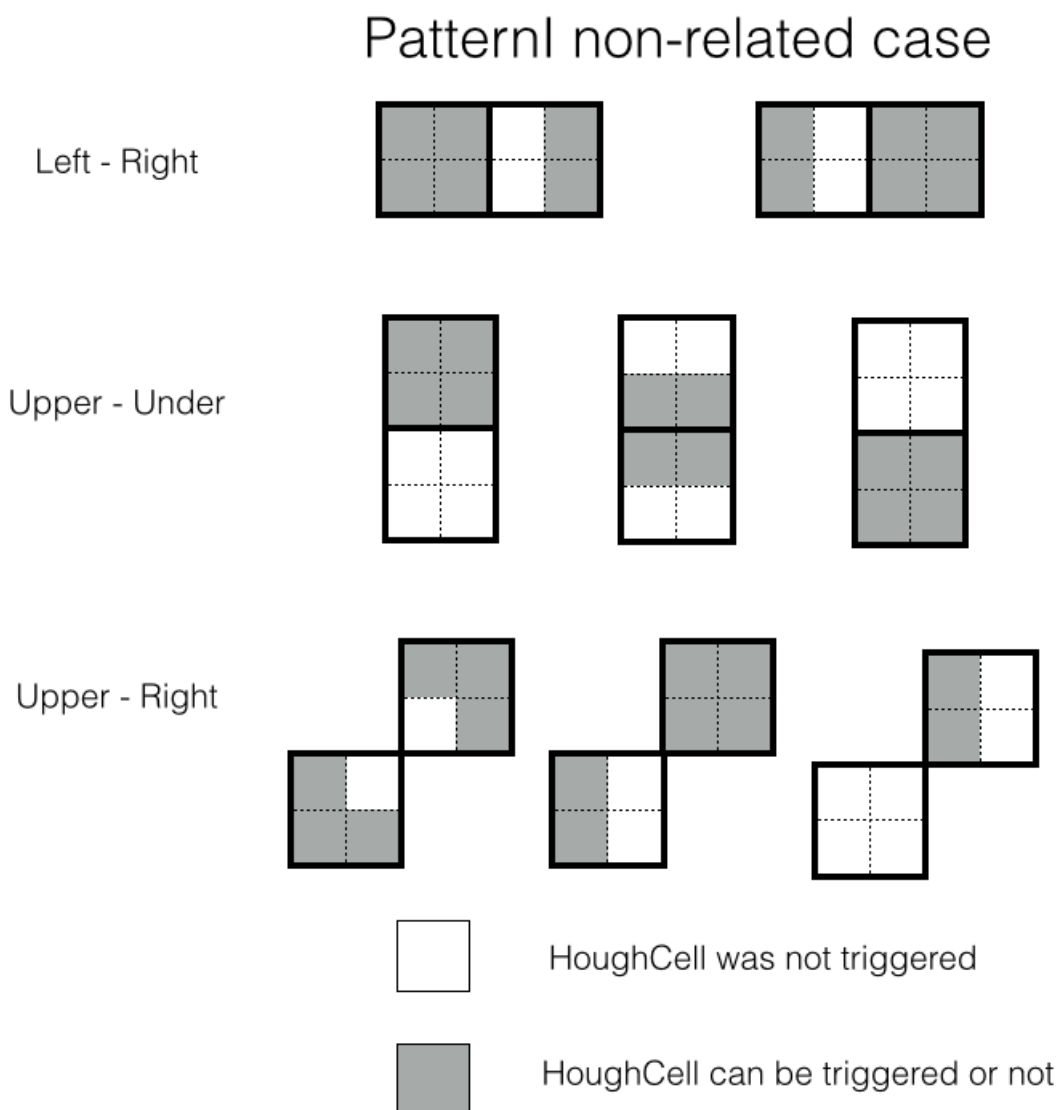


Figure 3.14: The relation comparison between each Pattern I is described here. Because it is easier to check the non-related case, we use this skill to decide our look-up-tables.

3.8 Center of Cluster

We find the center of Pattern II first and then find the center of Pattern I.

Six steps are used to find the center of Pattern II.

- Step 1 Select a Pattern II.
- Steps 2 Use the selection rules in the Figure 3.15 and decide the center of the Pattern II.
- Steps 3 Use the selection rules in the Figure 3.16 and decide the center of the Pattern I.

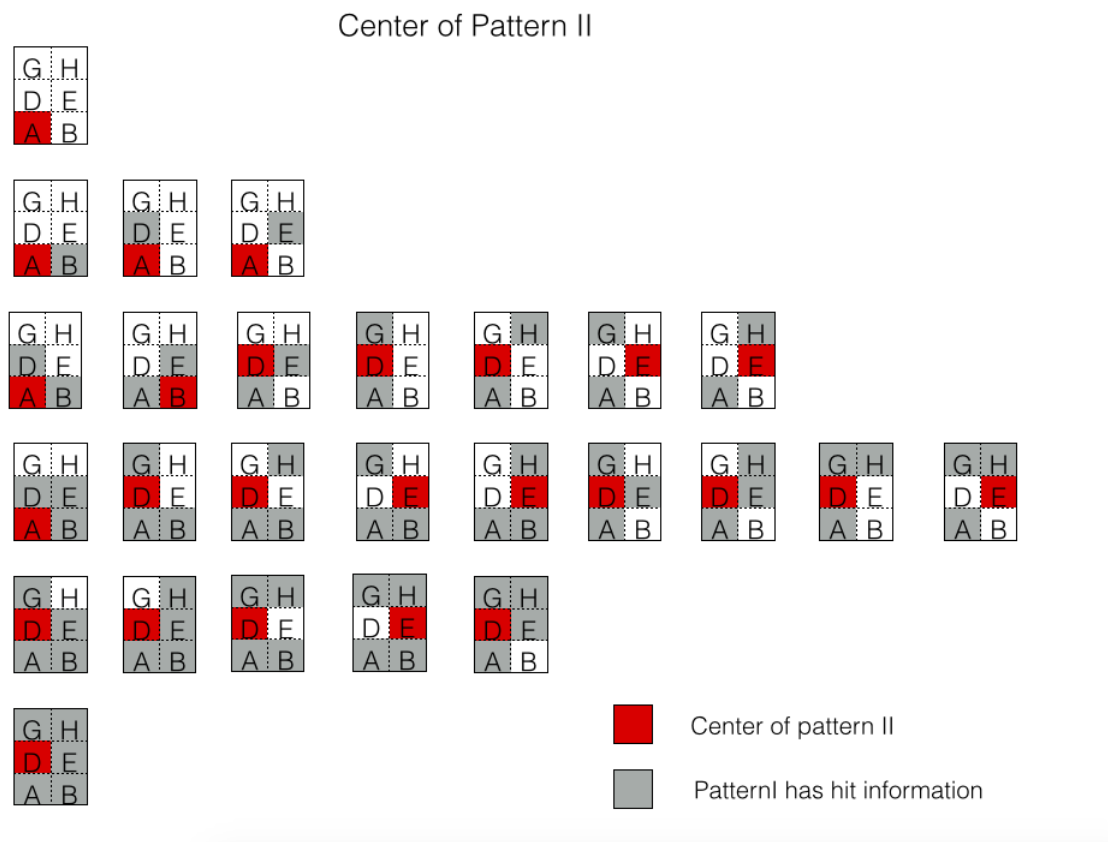


Figure 3.15: Use the selection rules and decide the center of the Pattern II.

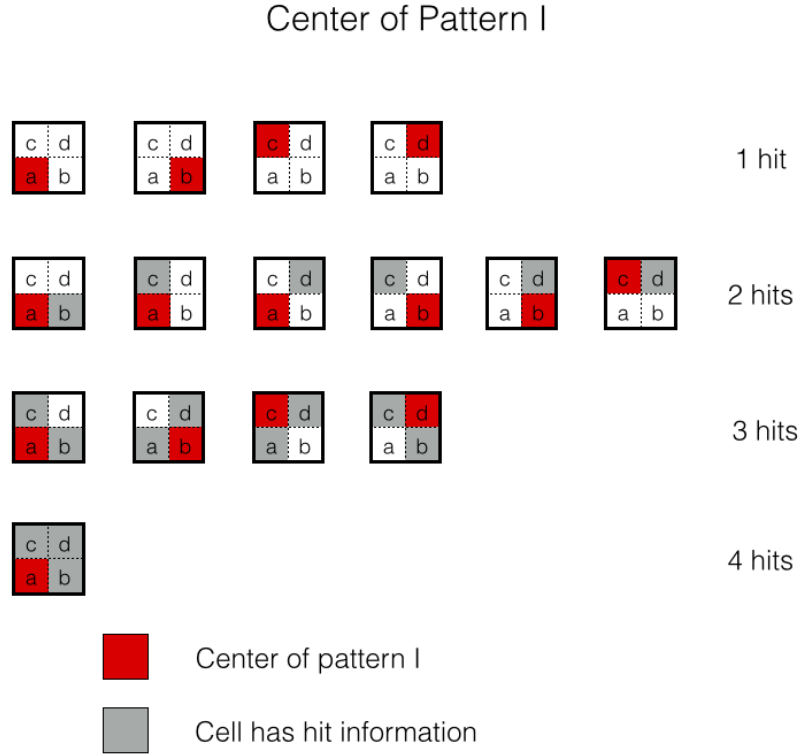


Figure 3.16: Use the selection rules and decide the center of the Pattern I.

particle

3.9 Efficiency in 2D logic

In order to know the performance of the track finding, we use the μ^- particle as the input. The transverse momentum is generated from 0.4 GeV to 0.5 GeV, 0.5 GeV to 1.0 GeV, 1.0 GeV to 2.0 GeV and 2.0 GeV to 5.0 GeV four parts. The number of input tracks is 1. In each case, we generate 1,000 times. Ideally, the input number of tracks will equal to the output number of tracks. The results are shown in the Figure 3.17. The efficiency is equal to 1, in high momentum, the doublecounting appears due to the HoughMapping in 2D logic.

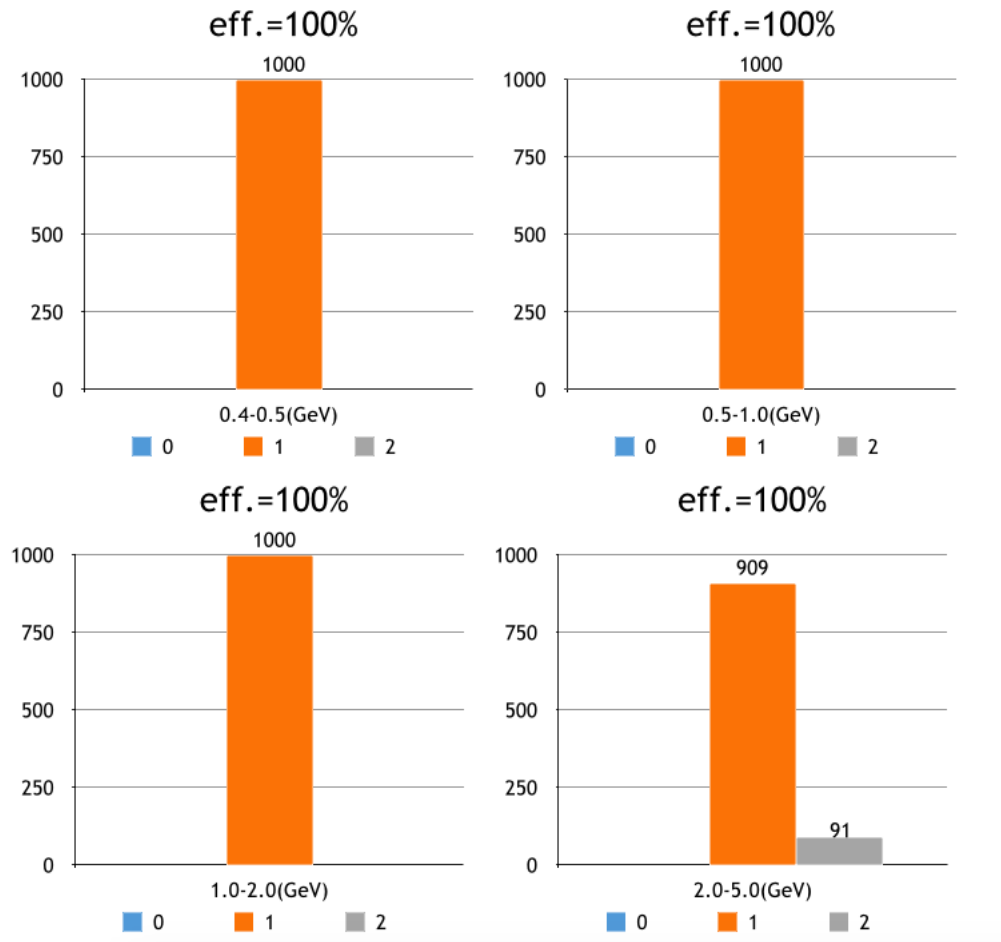


Figure 3.17: An efficiency of finding the track.

Chapter 4

The Fitter for 2D Full Tracker

4.1 Transforming track segment coordinates

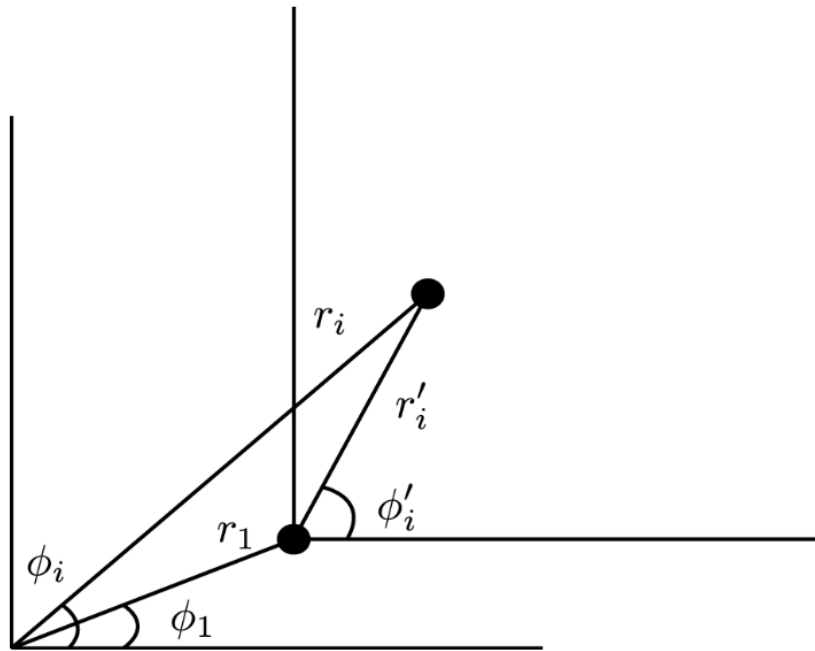


Figure 4.1: An example of track segment coordinate.

We want to move the coordinate system's origin to the first track segment \vec{T}_1 in order to doD fitter . We will indicate all values relative to the first segment as $'$ shown in the Figure (4.1). To calculate the

other 4 track segments relative to the first track segment, we do (4.1)

$$\vec{T}'_i = \vec{T}_i - \vec{T}_1 \quad (4.1)$$

Then r'_i and ϕ'_i will be

$$r'_i = |\vec{T}_i - \vec{T}_1| \quad (4.2)$$

$$= \sqrt{(x_i - x_1)^2 + (y_i - y_1)^2} \quad (4.3)$$

$$\phi'_i = \arctan\left(\frac{y_i - y_1}{x_i - x_1}\right) \quad (4.4)$$

After transforming the coordinates of the track segment we do 2D fitting.

4.2 2D fitter

The helix becomes a circle in 2D plane which passes thr origin in the transformed coordinate. When (a', b') is the coordinates of the center of the circle, R is the radius of the circle and (x'_i, y'_i) a point on the circle,

$$(x'_i - a')^2 + (y'_i - b')^2 = R^2 \quad (4.5)$$

$$x'^2_i - 2a'x'_i + y'^2_i - 2b'y'_i = 0 \quad (4.6)$$

$$r'^2_i - 2(a'x'_i + b'y'_i) = 0 \quad (4.7)$$

Since $x'_i = r'_i \cos \phi'_i$ and $y'_i = r'_i \sin \phi'_i$,

$$r_i'^2 - 2r'_i(a' \cos \phi'_i + b' \sin \phi'_i) = 0 \quad (4.8)$$

So the basic equation to do fitting is $r'_i = 2(a' \cos \phi'_i + b' \sin \phi'_i)$. We minimize χ^2 to do fitting where

$$\chi^2 = \sum_i^N \frac{[2(a' \cos \phi'_i + b' \sin \phi'_i) - r'_i]^2}{\sigma_i'^2} \quad (4.9)$$

$$\frac{\partial \chi^2}{\partial a'} = \sum_i^N \frac{2[2(a' \cos \phi'_i + b' \sin \phi'_i) - r'_i] \times 2 \cos \phi'_i}{\sigma_i'^2} = 0 \quad (4.10)$$

$$= \sum_i^N \frac{[2(a' \cos \phi'_i + b' \sin \phi'_i) - r'_i] \times \cos \phi'_i}{\sigma_i'^2} \quad (4.11)$$

$$= 2a' \sum_i^N \frac{\cos^2 \phi'_i}{\sigma_i'^2} + 2b' \sum_i^N \frac{\sin \phi'_i \cos \phi'_i}{\sigma_i'^2} - \sum_i^N \frac{r'_i \cos \phi'_i}{\sigma_i'^2} \quad (4.12)$$

$$\frac{\partial \chi^2}{\partial b'} = \sum_i^N \frac{2[2(a' \cos \phi'_i + b' \sin \phi'_i) - r'_i] \times 2 \sin \phi'_i}{\sigma_i'^2} = 0 \quad (4.13)$$

$$= \sum_i^N \frac{[2(a' \cos \phi'_i + b' \sin \phi'_i) - r'_i] \times \sin \phi'_i}{\sigma_i'^2} \quad (4.14)$$

$$= 2a' \sum_i^N \frac{\sin \phi'_i \cos \phi'_i}{\sigma_i'^2} + 2b' \sum_i^N \frac{\sin^2 \phi'_i}{\sigma_i'^2} - \sum_i^N \frac{r'_i \sin \phi'_i}{\sigma_i'^2} \quad (4.15)$$

$$2 \begin{bmatrix} \sum_i^N \frac{\cos^2 \phi'_i}{\sigma_i'^2} & \sum_i^N \frac{\sin \phi'_i \cos \phi'_i}{\sigma_i'^2} \\ \sum_i^N \frac{\sin \phi'_i \cos \phi'_i}{\sigma_i'^2} & \sum_i^N \frac{\sin^2 \phi'_i}{\sigma_i'^2} \end{bmatrix} \begin{bmatrix} a' \\ b' \end{bmatrix} = \begin{bmatrix} \sum_i^N \frac{r'_i \cos \phi'_i}{\sigma_i'^2} \\ \sum_i^N \frac{r'_i \sin \phi'_i}{\sigma_i'^2} \end{bmatrix} \quad (4.16)$$

$$\begin{aligned} 2 \begin{bmatrix} \sum_i^N \frac{\cos^2 \phi'_i}{\sigma_i'^2} & \sum_i^N \frac{\sin \phi'_i \cos \phi'_i}{\sigma_i'^2} \\ \sum_i^N \frac{\sin \phi'_i \cos \phi'_i}{\sigma_i'^2} & \sum_i^N \frac{\sin^2 \phi'_i}{\sigma_i'^2} \end{bmatrix}^{-1} &= \frac{1}{(\sum_i^N \frac{\cos^2 \phi'_i}{\sigma_i'^2})(\sum_i^N \frac{\sin^2 \phi'_i}{\sigma_i'^2}) - (\sum_i^N \frac{\sin \phi'_i \cos \phi'_i}{\sigma_i'^2})^2} \\ &\times \begin{bmatrix} \sum_i^N \frac{\sin^2 \phi'_i}{\sigma_i'^2} & - \sum_i^N \frac{\sin \phi'_i \cos \phi'_i}{\sigma_i'^2} \\ - \sum_i^N \frac{\sin \phi'_i \cos \phi'_i}{\sigma_i'^2} & \sum_i^N \frac{\cos^2 \phi'_i}{\sigma_i'^2} \end{bmatrix} \end{aligned} \quad (4.17)$$

$$\begin{aligned}
\begin{bmatrix} a' \\ b' \end{bmatrix} &= \frac{1}{2[(\sum_i^N \frac{\cos^2 \phi'_i}{\sigma_i'^2})(\sum_i^N \frac{\sin^2 \phi'_i}{\sigma_i'^2}) - (\sum_i^N \frac{\sin \phi'_i \cos \phi'_i}{\sigma_i'^2})^2]} \\
&\times \begin{bmatrix} \sum_i^N \frac{\sin^2 \phi'_i}{\sigma_i'^2} & - \sum_i^N \frac{\sin \phi'_i \cos \phi'_i}{\sigma_i'^2} \\ - \sum_i^N \frac{\sin \phi'_i \cos \phi'_i}{\sigma_i'^2} & \sum_i^N \frac{\cos^2 \phi'_i}{\sigma_i'^2} \end{bmatrix} \begin{bmatrix} \sum_i^N \frac{r'_i \cos \phi'_i}{\sigma_i'^2} \\ \sum_i^N \frac{r'_i \sin \phi'_i}{\sigma_i'^2} \end{bmatrix} \\
&= \begin{bmatrix} \frac{(\sum_i^N \frac{\sin^2 \phi'_i}{\sigma_i'^2})(\sum_i^N \frac{r'_i \cos \phi'_i}{\sigma_i'^2}) - (\sum_i^N \frac{\sin \phi'_i \cos \phi'_i}{\sigma_i'^2})(\sum_i^N \frac{r'_i \sin \phi'_i}{\sigma_i'^2})}{2[(\sum_i^N \frac{\cos^2 \phi'_i}{\sigma_i'^2})(\sum_i^N \frac{\sin^2 \phi'_i}{\sigma_i'^2}) - (\sum_i^N \frac{\sin \phi'_i \cos \phi'_i}{\sigma_i'^2})^2]} \\ - \frac{(\sum_i^N \frac{\sin \phi'_i \cos \phi'_i}{\sigma_i'^2})(\sum_i^N \frac{r'_i \cos \phi'_i}{\sigma_i'^2}) - (\sum_i^N \frac{\cos^2 \phi'_i}{\sigma_i'^2})(\sum_i^N \frac{r'_i \sin \phi'_i}{\sigma_i'^2})}{2[(\sum_i^N \frac{\cos^2 \phi'_i}{\sigma_i'^2})(\sum_i^N \frac{\sin^2 \phi'_i}{\sigma_i'^2}) + (\sum_i^N \frac{\sin \phi'_i \cos \phi'_i}{\sigma_i'^2})^2]} \end{bmatrix} \quad (4.18)
\end{aligned}$$

There are 5 common compiments in these equations which are

$$(\sum_i^N \frac{\sin^2 \phi'_i}{\sigma_i'^2}), (\sum_i^N \frac{\cos^2 \phi'_i}{\sigma_i'^2}), (\sum_i^N \frac{\sin \phi'_i \cos \phi'_i}{\sigma_i'^2}), (\sum_i^N \frac{r'_i \sin \phi'_i}{\sigma_i'^2}), (\sum_i^N \frac{r'_i \cos \phi'_i}{\sigma_i'^2}).$$

Using these components we can calculate a' and b' .

4.3 Transforming back 2D fitter results

To move back to the original coordinates system, we add \vec{T}_1 to the circle center vector $\vec{P}'(a', b')$ as

$$\vec{P} = \vec{P}' + \vec{T}_1$$

$$a = a' + x_1$$

$$b = b' + y_1$$

The radius of the circle is

$$R = \sqrt{a'^2 + b'^2}$$

4.4 Classes for Cpp to VHDL

We appreciate Jae-Bak who developed classes which write VHDL. In order to do the same complicated calculation in VHDL, we may need the look-up-table for trigonometry and multiplying those compoment.

In the Figure 4.2, it shows the fitter2D was developed using the framework.

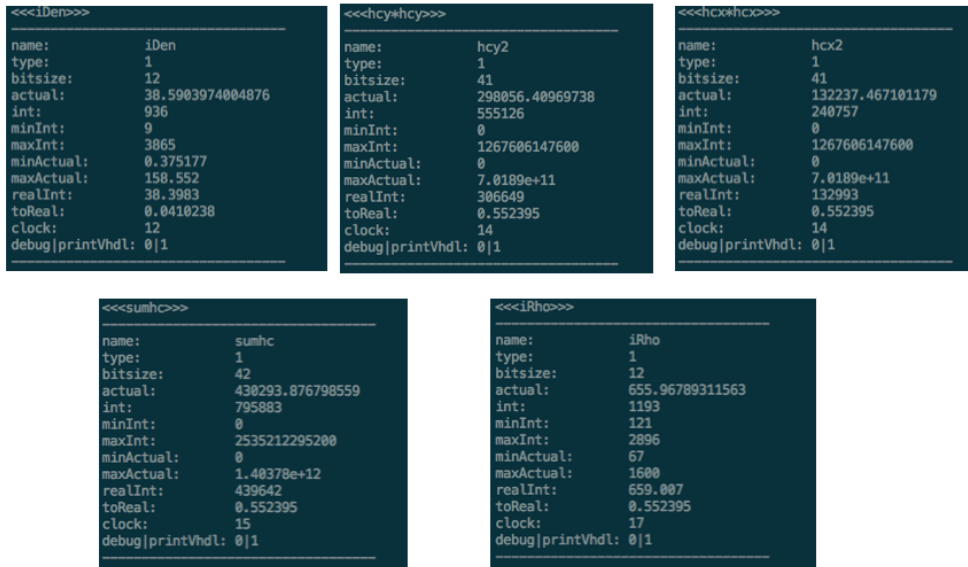


Figure 4.2: Debugging text for one track.

4.5 Histogram of Pt and Phi

We use the μ^- particle as the input particle. The momentum is generated from 0.4 - 5.0 GeV. The number of track is 1 and we generate 1,000 times. The results are shown in the Figure 4.3 and 4.5.

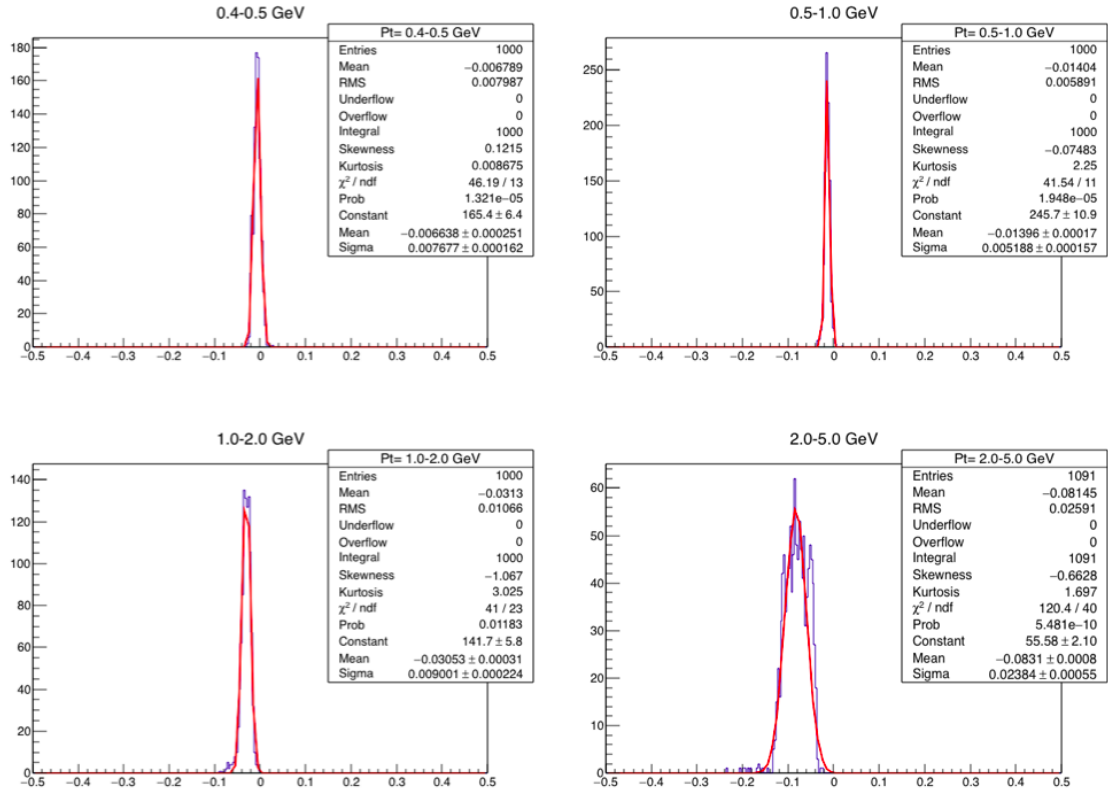


Figure 4.3: The histogram of Pt. In each case, we generated 1,000 times. The momentum is from 0.4 to 5.0 GeV.

In the Figure 4.3, there is a tendency to the value which is smaller than 0. It is due to the formula we use. We can see the resolution in Figure 4.4, the ideally resolution of Hough finding is five percent. In reality, Hough finder get the resolution around twenty percent so we need the fitter which can get better performance in finding the track.

Pt(GeV)	$\sigma(\%)$
0.4-0.5	0.77
0.5-1.0	0.52
1.0-2.0	0.9
2.0-5.0	2.3

Figure 4.4: The resolution of Pt. The momentum is from 0.4 to 5.0 GeV..

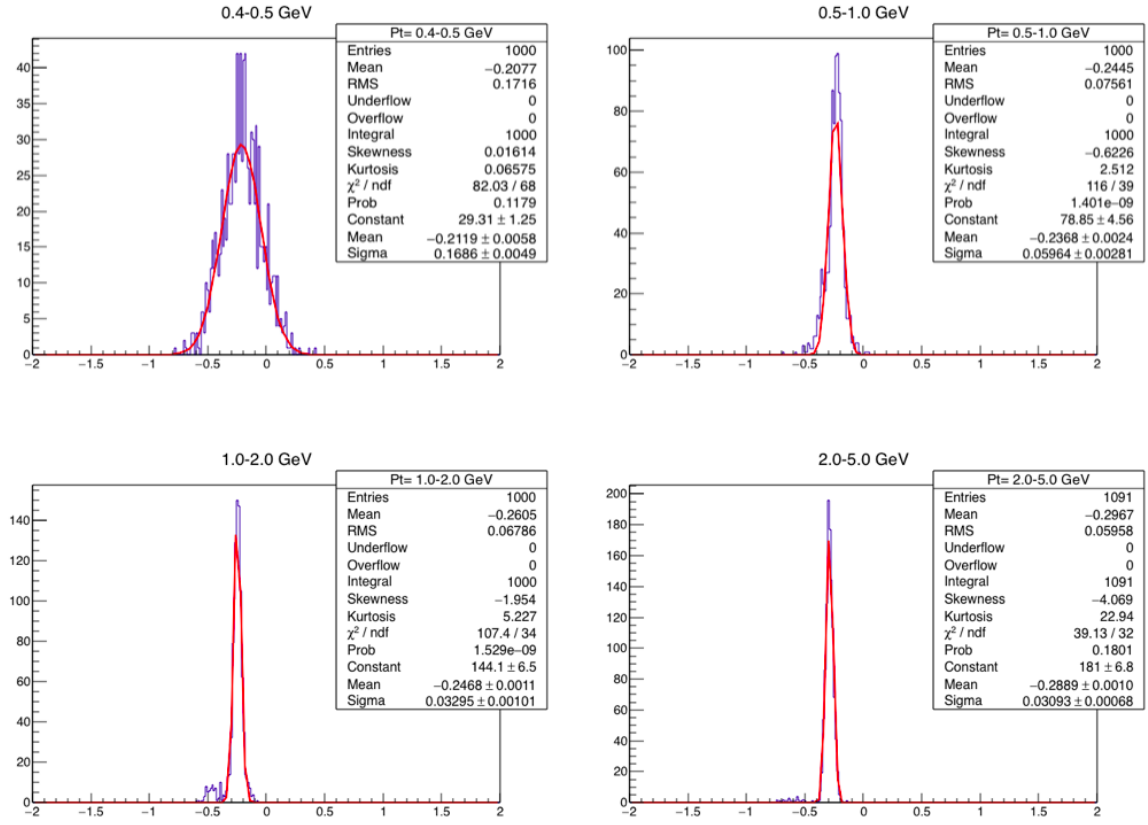


Figure 4.5: The histogram of Φ . In each case, we generated 1,000 times. The momentum is from 0.4 to 5.0 GeV.

Chapter 5

Summary

We modified the pattern size in Hough cell finding and get better efficiency by changing Hough cell mapping.

The fitter for 2D tracker works well in the simulation.

Bibliography

- [1] <http://legacy.kek.jp/intra-e/index.html>
- [2] Kobayashi M. and Maskawa T., CP Violation in the Renormalizable Theory of Weak Interaction, Prog. Theor. Phys. 49, 652657, (1973).
- [3] <http://www.nobelprize.org/>
- [4] Belle II collaboration, Belle II Technical Design Report, KEK-REPORT-2010-1, July 2010.
- [5] <http://legacy.kek.jp/intra-e/feature/2010/BelleIICDCDesign.html>
- [6] http://en.wikipedia.org/wiki/Hough_transform